Coordination complexes of thiazyl rings. Synthesis, structure and DFT computational analysis of CpCr(CO)$_x$ (*x* = 2,3) complexes of fluorinated and non-fluorinated 1λ^3-1,2,4,6-thiatriazinyls, with differing Cr—S bond orders.

Chwee Ying Ang, Seah Ling Kuan, Geok Kheng Tan, Lai Yoong Goh, Tracey L. Roemmele, Xin Yu and René T. Boeré

Chwee Ying Ang, Seah Ling Kuan, Geok Kheng Tan, Lai Yoong Goh[#]. Department of Chemistry, National University of Singapore, Kent Ridge, Singapore 117543.

Tracey L. Roemmele, Xin Yu and René T. Boeré. Department of Chemistry and Biochemistry *and* the Canadian Centre for Research in Advanced Fluorine Technologies, University of Lethbridge, 4401 University Dr. W, Lethbridge, AB, Canada T1K 3M4.

Corresponding authors:René T. Boeré (e-mail: boere@uleth.ca). Lai Yoong Goh (gohly@utar.edu.my; chmgohly1@hotmail.com).

[#] Present affiliation: International Collaborative Partner, UTAR Global Research Network, Universiti Tunku Abdul Rahman, 31900 Kampar, Perak, Malaysia.

Dedication: This paper is part of the special issue for the centennial of chemical publications from Western University and honours the mentorship of Prof. Christopher J. Willis, a pioneer in the use of fluorinated ligands in coordination chemistry.

Abstract: Reaction of [3,5-Ph$_2$-C$_2$N$_3$S]$_2$ with [CpCr(CO)$_3$]$_2$ in toluene at RT forms an adduct *via* a Cr—S bond, formulated as CpCr(CO)$_3$SN$_3$C$_2$Ph$_2$, which has fitting NMR, IR and combustion analysis data. The structure was determined by a single-crystal X-ray structure diffraction study (P2$_1$/*n*, *a* = 8.4611(17) Å; *b* = 20.509(4) Å, *c* = 11.757(2) Å, β = 104.453(7)°). The Cr—S bond-length = 2.4908(11) Å corresponds to a bond-order of 1.0 from > 90 values for CpCr(CO)$_x$ or Cp*Cr(CO)$_x$ moieties (*x* = 2,3) bonded to S which are used to establish a Pauling-type bond order scale specific to this class of compounds. Similar reactions of fluorinated thiatriazinyls derived from [3-Ph-5-CF$_3$-C$_2$N$_3$S]$_2$ or [4-MeOC$_6$H$_4$-5-CF$_3$-C$_2$N$_3$S]$_2$ are accompanied by the loss of CO to produce CpCr(CO)$_2$SN$_3$C$_2$PhCF$_3$ (P$\bar{1}$, *a* = 8.0929(8) Å; *b* = 10.3160(10) Å, *c* = 11.2405(11), α = 70.032(2)°, β = 72.076(2)°, γ = 82.375(2)°) and CpCr(CO)$_2$SN$_3$(CCF$_3$)(C$_6$H$_4$OCH$_3$) (P2$_1$/*c*, *a* = 8.1311(7) Å; *b* = 24.284(2) Å, *c* = 9.1025(8) Å, β = 97.218(2)°), also fully characterized by spectroscopy and crystallography. Their measured Cr—S bond-lengths, 2.2987(14) Å and 2.2965(11) Å, correspond to bond orders of 1.5. (U/R)B3PW91/6-311+G(2df,2p)//B3PW91/6-31G(2d,p) hybrid DFT calculations show that the tricarbonyl complex has an unusual σ bond. However, the dicarbonyl complexes of the fluorinated thiatriazinyls are π-bonded.

Résumé: La réaction de [3,5-Ph$_2$-C$_2$N$_3$S]$_2$ avec [CpCr(CO)$_3$]$_2$ dans du toluène à la température ambiante donne un produit d'addition par l'intermédiaire d'une liaison Cr—S, formulée comme CpCr(CO)$_3$SN$_3$C$_2$Ph$_2$, pour qui le RMN, IR et des données d'analyse de combustion sont juste. La structure a été déterminée par un étude de diffraction monocristalline des rayons-X (P2$_1$/*n*, *a* = 8.4611(17) Å; *b* = 20.509(4) Å, *c* = 11.757(2) Å, β = 104.453(7)°). La longueur du liaison Cr—S, 2.4908(11) Å, correspond à un ordre de liaison de 1,0 à partir de > 90 valeurs pour CpCr(CO)$_x$ or Cp*Cr(CO)$_x$ groupements (*x* = 2,3) lié à S qui sont utilisés pour établir une échelle de Pauling d'ordre du liaison spécifique pour cette classe de composés. Des réactions similaires en utilisant les thiatriazinyls fluorés dérivés de [3-Ph-5-CF$_3$-C$_2$N$_3$S]$_2$ ou [4-MeOC$_6$H$_4$-5-CF$_3$-C$_2$N$_3$S]$_2$ sont accompagnés par la perte de CO pour produire CpCr(CO)$_2$SN$_3$C$_2$PhCF$_3$ (P$\bar{1}$, *a* = 8.0929(8) Å; *b* = 10.3160(10) Å, *c* = 11.2405(11), α = 70.032(2)°, β = 72.076(2)°, γ = 82.375(2)°) and CpCr(CO)$_2$SN$_3$(CCF$_3$)(C$_6$H$_4$OCH$_3$) (P2$_1$/*c*, *a* = 8.1311(7) Å; *b* = 24.284(2) Å, *c* = 9.1025(8) Å, β = 97.218(2)°), également entièrement caractérisé par spectroscopie et de la cristallographie. Leurs longueurs des liaisons Cr—S, 2.2987(14) Å et 2.2965(11) Å, correspond à un ordre de liaison de 1.5. Calculs TFD hybrides (U/R)B3PW91/6-311+G(2df,2p)//B3PW91/6-31G(2d,p) montrer que le complexe de tricarbonyl a une liaison inhabituelle σ, mais les complexes thiatriazinyls fluorés sont liés en façon π.

Key words: multiple-bonds, thiazyl radicals, trifluoromethyl, chromium-sulfur bonds, chromium-nitrogen bonds, π-bonding, single crystal X-ray crystallography, DFT calculations

Mots-clés: liaisons multiple, radicaux thiazyle, trifluorométhyle, liaisons chrome-soufre, liaisons chrome-azote, liaisons π, diffraction monocristalline des rayons-X, calculs TFD
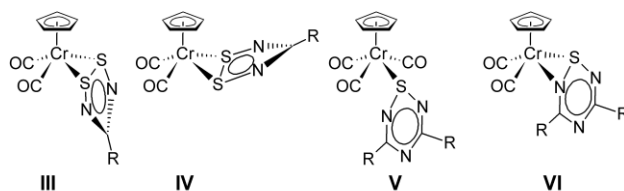
Introduction

A major topic in modern main group chemistry is the degree to which elements other than carbon can partake in multiple bonding and unsaturation.[1-17] Thus, all the properties considered for carbocycles: ring-strain, geometry (flat *vs.* puckered), aromaticity and anti-aromaticity have been sought amongst ring compounds of the other *p*-block elements. A recurring theme has been whether or not a given main group species can form π-complexes with low-valent transition metals.[18-24] Carbon itself forms the ubiquitous η^n–cyclopentadienyl coordination compounds with almost all the metal ions in the periodic table, with *n* ranging from 1 − 5, but with the latter by far the most common. Thus, it takes a certain mental effort to recall that the alternative, that is, metal insertion into C–C bonds giving "metallocyclobenzenes", is entirely plausible. For C_5 rings this alternative is often, but not always, less thermodynamically stable than forming a π-complex.[25,26] There are well-documented cases wherein *cyclo*-MC$_5$R$_5$ complexes (**I**) isomerize to (η^5–C$_5$R$_5$)M (**I'**).[27] When it comes to unsaturated thiazyl (-S=N-) ring compounds, the evidence amassed thus far is that insertion (by oxidative addition) dominates.[28-30] For example, the unsaturated 6π-electron heterocycle 3,4-(dicyano)-1,2,5-thiadiazole is not known to form any η^5-π complexes (**II**). Instead, it undergoes a clean insertion reaction with the Pt(0) complex (Ph$_3$P)$_2$Pt(C$_2$H$_4$) to form the *cyclo*-MSN$_2$C$_2$(CN)$_2$ ring compound (**II'**).[31] Oxidative addition also predominates for metal complexes of 1,2,3,5-dithiadiazoyl (DTDA) radicals, RCN$_2$S$_2$,[30,32] although this class of thiazyl radicals affords a greater variety of adduct geometries, including metallacycles akin to **II'** *that retain paramagnetism* as well as larger clusters that are found both as diamagnetic and paramagnetic species (representative structures are shown as A − E in Chart 2 of ref. 33).
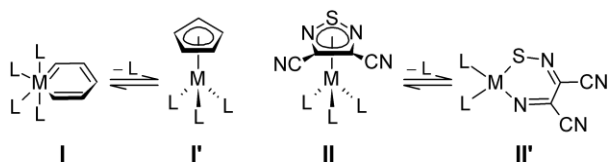
By contrast, we recently reported the first η^2-RCN$_2$S$_2$ π complexes (**III** and **IV**) with CpCr(CO)$_2$ which have been isolated in *exo* and *endo* configurations, respectively.[33-35] A signature feature of **III** and **IV** is that, in contrast to all previous complexes with low-valent metals, the S—S separation is almost unchanged from that of the dimeric radicals that have been crystallographically analyzed. Thus, oxidative addition – the dominant reaction of low-valent transition metals towards element-element

bonds – is avoided for the first time for any thiazyl ring compounds. Moreover, the metal attaches perpendicularly to the ring plane, with the ligand acting as a 3*e* donor *via* the S—S bond.

The generality of this result was supported by a subsequent communication from our laboratories that reported similar complexes of 1,2,4,6-thiatriazinyl radicals with CpCr(CO)$_x$ (x = 2,3) fragments.[36] This report introduced two new modalities: first, the η^1-adduct **V** retains all three carbonyl groups on Cr and is unambiguously bonded through the ring S atom. Second, the η^2-adduct **VI** has lost one carbonyl group but is now bonded to a ring S=N bond, while in both cases the metal attaches perpendicularly to the ring plane, as generally expected for π coordination.

Preuss and co-workers have shown that intact thiazyl radicals can form co-planar σ-complexes via a ring N atom with coordinatively saturated, non-oxidizing M(hfac)$_2$ complexes of Cu(II), Ni(II) and Mn(II) when an adjacent donor atom is available (i.e. a chelating "bipyridyl" type geometry – structures F and G in Chart 2 of ref. 33).[29] Previously, Hursthouse *et al*. reported on the preparation by salt-metathesis routes of complexes of Ti, Zr, Mo, Ni and Ru in middle-oxidation states containing the Ph-S=N-^{t}Bu unit, but these structures have very short metal-nitrogen and rather long metal-sulfur bonds, and are therefore contraindicative of π bonding to sulfur,[37-39] whereas structures of type **VI** are not distorted in this fashion. Thus, there seems to be something quite special about the [CpCr(CO)$_{2,3}$]$^\bullet$ metal environment that results in mild chemical interactions with thiazyl radicals. This same metal environment supports a vast range of interactions to main group E—E' bonds in a plethora of coordination environments and in a range of formal oxidation states.[40-61]

Herein we report further on the complexes **V** and **VI**, including full synthetic details and another example of type **VI**. The chemical behaviour, as well as the contrast between the structures of the two reagents, i.e. the σ dimer [CpCr(CO)$_3$]$_2$ and the diffuse π-bonded face-to-face main group heterocyles, have been thoroughly investigated using DFT computational methods. This work is anchored in thorough structural evidence from crystallography for the recently published trifluoromethyl 1λ^3-1,2,4,6-thiatriazinyls,[62] electrochemical studies on these heterocyclic radicals and the Cr reagent,[63] the structural characterisation of the products of type **V** and **VI** reported here and EPR characterization of thiatriazinyls.[62,64] This provides an intriguing opportunity to examine the nature of the bonding between

(radical) thiazyl monomers to [CpCr(CO)$_3$]$^{\bullet}$ organometallic radicals and the origins of the suppression of oxidative addition.

Results and discussion

Synthesis.

Scheme 1 Reaction of [CpCr(CO)$_3$]$_2$, **1**, with the symmetrical thiatriazinyl **2**
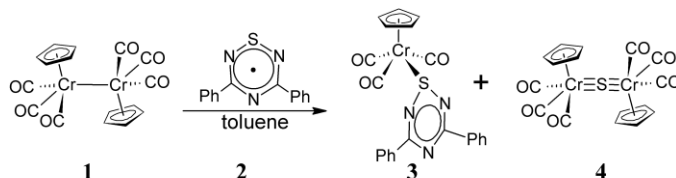

The reaction of [CpCr(CO)$_3$]$_2$,[65] **1**, with the symmetrical diphenylthiatriazinyl radical [66,67] **2** in toluene at ambient temperature (Scheme 1) affords a mixture of the new thiatriazinyl complex **3** and the known complex [CpCr(CO)$_2$]$_2$S,[40,42,46] **4**, which were separated by fractional crystallization. The progress of the reaction can be conveniently monitored by ^{1}H-NMR because the cyclopentadienyl signal of **1**, which is in equilibrium with the monomeric organometallic radical [CpCr(CO)$_3$]$^{\bullet}$, can be observed as a line-broadened peak despite the presence of the radicals in solution. Such spectra show that **3** forms slowly as **1** is consumed, but subsequently decomposes to **4**. The optimal yield is obtainable from careful monitoring of the NMR integrations of the three components, and occurs at approximately the four-hour mark.

Scheme 2 Reactions of [CpCr(CO)$_3$]$_2$, **1**, with trifluoromethyl thiatriazinyls **5a,b**
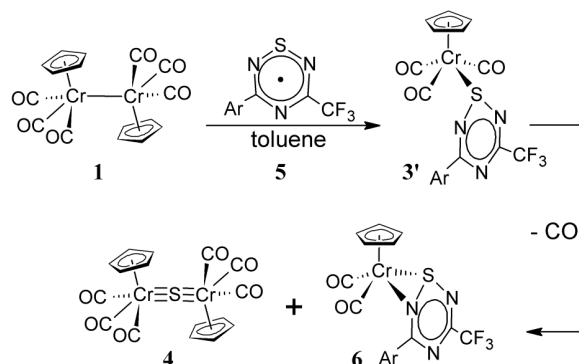
In similar reactions of **1** with the trifluoromethyl thiatriazinyls **5a,b** [Ar = C$_6$H$_5$ (a); Ar = 4-CH$_3$OC$_6$H$_4$ (b)],[62] only **4** and the new complexes **6a,b** were isolated (Scheme 2). In such reactions, aliquots taken for NMR show the initial formation of an intermediate that later transforms into the isolated product. This may indicate that the first step of the reaction forms an η^1-complex with CpCr(CO)$_3$, indicated as **3'** in Scheme 2, but isolating such a species has thus far not been possible. Over time, this signal gives way to

the final products, **6a,b** which could be isolated by low-temperature crystallization. A precedent for the conversion of such an intermediate has been established in the reaction of **1** with tetraalkyldithiuram disulfides where the low-temperature (−29 °C) products are monodentate $CpCr(CO)_3$-thiocarbonates, which at ambient temperatures convert quantitatively to bidentate $CpCr(CO)_2$-thiocarbonates with loss of one CO group.[49] Just as in the reactions that produce **3**, **6a,b** are produced as mixtures along with some **4**, and the separation is also by fractional crystallization. The structures of the thiatriazinyl complexes **3** and **6a,b** have been determined by single-crystal X-ray diffraction (Tables 2 - 5; Figures 1 - 3).

Figure 1 Displacement ellipsoids plot (40% probability) of **3** as found in the crystal, showing the atom numbering scheme, the perpendicular orientations of ring and metal, as well as the long Cr—S bond. The dihedral angle for rotation about this bond is defined as C21-Cr1-S1-N2 (see text).
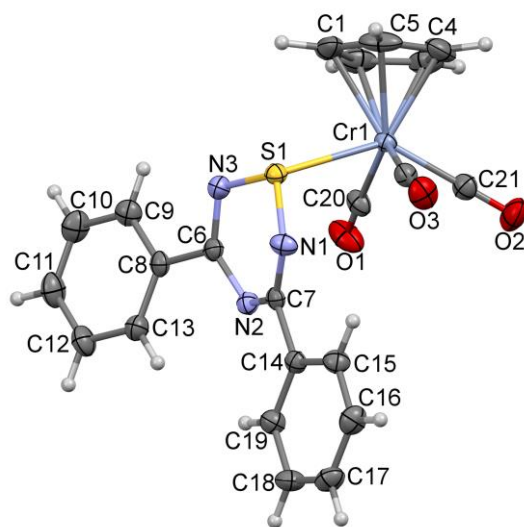
Crystallography.

A plot of the molecular structure of thiatriazinyl complex **3** is depicted in Figure 1. The Cr—S bond is long and very close to that expected for a single bond (see below for details), the thiatriazinyl ring remains intact (no evidence of oxidative addition occurring) and the metal is convincingly oriented perpendicularly to the mean plane of the heterocycle. As already noted in our communication,[36] the ring in complex **2** is distorted into a slight boat conformation that is intermediate between that found in the neutral **2₂** dimer [67] and the (protonated) anion **2H**.[68] Similarly, the bond distances within the ring are found to be intermediate, and both structural features are consistent with the coordinated ring bearing approximately a −0.5 unit charge. From a consideration of the 18e rule, the ligand acts as a 1*e* donor towards $CpCr(CO)_3$, consistent with the formation of a single bond to the ring. Further considerations of

the mode of bonding as well as comparison of metric data are taken up below after discussing the computational results.
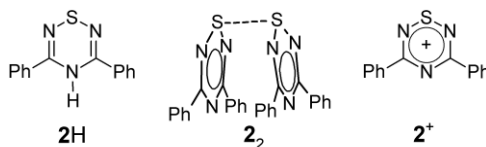

2H 2₂ 2⁺

Figure 2 Displacement ellipsoids plot (20% probability) of **6a** as found in the crystal, showing the atom numbering scheme, the short Cr—S and Cr—N bonds and the perpendicular orientations of ring and metal with *exo* orientation of the thiatriazinyl w.r.t. the Cp rings.
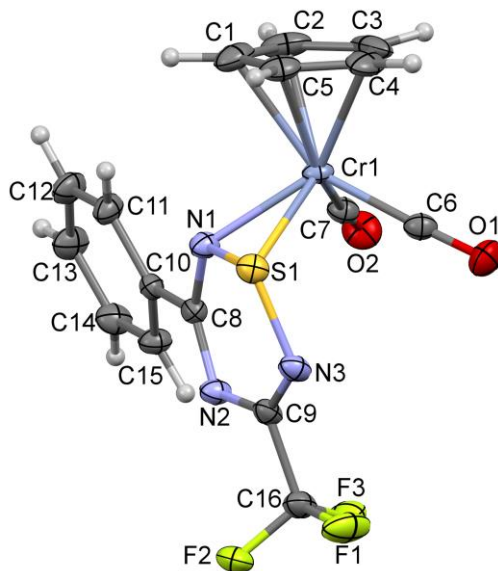
The molecular structure of complex **6a** is depicted in Figure 2. It shares with **3** the *exo* orientation and perpendicular bonding of the metal to the ring, but differs in that there are now only two carbonyl groups bonded to the metal and consequently, the metal is coordinated to both S1 and N1, with a remarkably short S to Cr bond. From a consideration of the 18e rule, the ligand acts as a 3*e* donor towards CpCr(CO)$_2$. This bonding mode is thus very similar to what is observed in the case of the aryl η^2-DTDA complexes of type **III**.[33-35] In the latter case, we were able to show that such complexes in solution are in dynamic exchange between the *exo* (major) and *endo* (minor) isomers in solution, while by using different remote substituents on the aryl ring, either one or the other crystallizes preferentially. However, for **6a,b** only the *exo* form has yet been isolated and the solution behaviour seems to be dominated by a single species according to the NMR evidence.

Figure 3 Displacement ellipsoids plot (40% probability) of **6b** as found in the crystal, also in *exo* orientation, showing the atom numbering scheme for the asymmetric unit and also showing the short $S^{\delta+}\cdots N^{\delta-}$ contacts that link two complexes side-by-side into centrosymmetric pairs within the crystal lattice (dashed blue tubes).
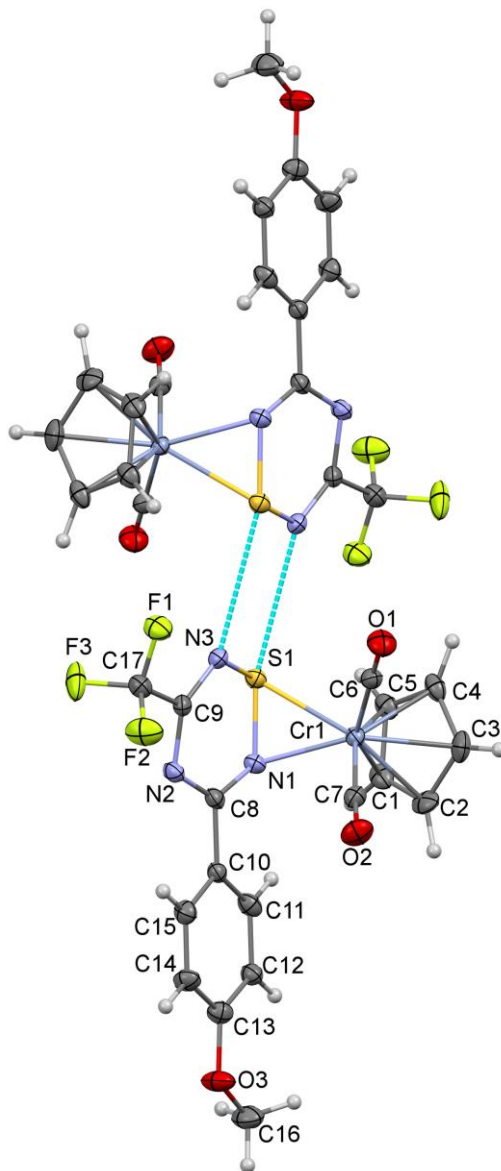
The molecular structure of **6b** (Figure 3) as found in the crystal has an *exo* orientation very similar to that found in **6a**. It differs from the latter in its extended structure insofar as the lattice shows short intermolecular contacts $S^{\delta+}\cdots N^{\delta-}$ between two molecules aligned side-by-side, a motif which is quite typical amongst thiazyl heterocycles.[28,69] Indeed, the parent radical **5b** (Figure 4) is associated in the solid state both as a face-to-face π dimer, and as a somewhat skewed side-by-side pair with a second such π dimer.[62] In **5b**, the pair-wise contacts are N20···S10, 2.941(1); S20···N20, 3.320(1) and S20···N10 3.341(1) Å, which are shorter than the sums of their v.d.Waals' radii ($\sum r_{vdW}$) by 0.41, 0.03 and 0.01 Å,

respectively, so that only the first represents a strong contact. The centrosymmetric S1···N3 contact of 3.253(4) Å in the crystal structure of **6b** is 0.1 Å < $\sum r_{vdW}$, weaker than that found for the parent heterocycle, but still significant. It should also be noted that the crystal structures of both **6a** and **6b** are tightly packed, with numerous F···H, O···H, O···C and C···C contacts that are < $\sum r_{vdW}$.

Figure 4 Displacement ellipsoids plot (40% probability) of the centrosymmetric pairs-of-dimers structure corresponding to the unit cell contents in the crystal structure of **5b**, showing the short contact between sulfur atoms (yellow broken tubes) in the face-to-face π-bonded dimer as well as the short $S^{\delta+}···N^{\delta-}$ contacts (gray broken tubes) that link two such dimers into offset pairs (for full structure details see ref. 62).
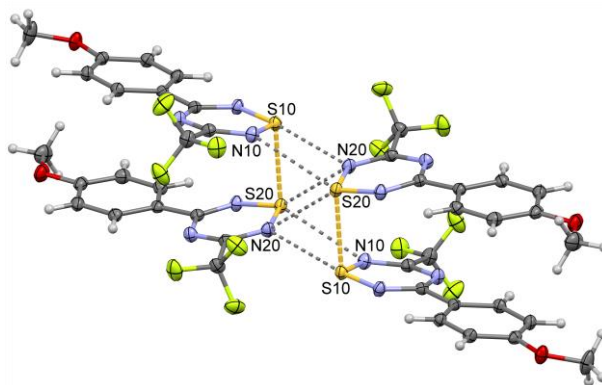
Bond order.

Given the unprecedented structures of complexes **3**, **6a,b** and the related dithiadiazolyl complexes of type **III** and **IV**, it can be challenging to make sense of the geometrical parameters. What are we to make of the significantly different Cr—S distances of 2.4908(11) Å in **3**, 2.2987(14) Å in **6a** and 2.2965(11) Å in **6b**, or for that matter, what do the similar Cr—N distances of 2.100(4) Å and 2.098(3) Å in **6a** and **6b** signify?

By considering a body of results that has been generated almost entirely in one of our laboratories over several decades, it is now possible to define a bond length/bond order correlation for a wide variety of different Cr—S distances in chalcogen, chalcogen-carbon and chalcogen-pnictide adducts with CpCr(CO)$_x$ or Cp*Cr(CO)$_x$ moieties (x = 2,3). More than 90 relevant bond distances measured in over 40 crystal structure determinations are compiled in Table 1. In all, thirteen different structural types could be identified amongst these compounds, as listed in the table along with short descriptions. (Readers wishing greater structural details can consult representative molecular plots in the Supporting Information, or access the full structural details using the supplied Cambridge Structural Database (CSD) "refcodes".)[70] An analysis of this data is reported graphically in Figure 5. The value of a Cr—S single bond length is established in three different ways. First, the sums of the covalent radii as recently re-determined by Cordero, *et al.*[71] gives a value of 2.440 Å. Second, the structure types for which a single

bond is expected based on chemical intuition, specifically terminal thiolato derivatives of CpCr(CO)$_3$ (structures with refcodes MAKLOA, RATRIO AND XULGOY) have Cr—S bond distances of 2.4485(8),[44] 2.448(3) [47] and 2.4406(8) Å,[49] respectively. Lastly, the full distribution between 2.37 – 2.52 Å for structure types that provide the major Gaussian distribution in the histogram (Figure 5), rejecting two outliers > 2.52, results in a mean value of 2.45(4) Å. All of these determinations are in excellent agreement; for consistency with the literature the value based on covalent radii is used in further calculations. Three structure determinations (refcodes: SPDCC, SPDCC01 AND YODZAS) exist for complex **4** and a close analog.[40-42] This class of compounds contains linear CrSCr bridging units with Cr≡S triple bonds (through a synergistic combination of donation and back-donation) and the mean value from this data subset is 2.074(3) Å for the triple bond. Using these two anchoring values, a Pauling-type bond order calculation is undertaken based on the approach used by Lendvay,[72] as defined in Eqn. 1 where n is the bond order, R is the experimental bond length, and R_0 is the standard single bond distance.

$$n = e^{-\left[\frac{(R-R_0)}{b}\right]}; \quad (b = 0.34)$$

Equation 1

The value of 0.34 obtained here for the scaling factor b is very consistent with other Pauling bond order determinations using the Lendvay approach.[72]

Figure 5 Graphical analysis of Cr–S bond distances from a compilation of all structures reported in the CSD wherein a CpCr(CO)$_x$ moiety is bound to at least one sulfur atom. For further details, see text and Table 1.
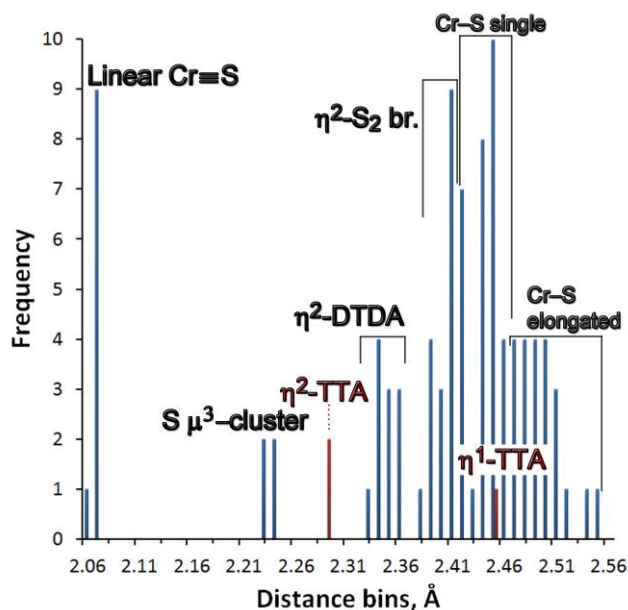
It is possible to interrogate the bond distance histogram in Figure 5 in greater detail. For the longer distances, a true Cr-S single bond distance of 2.444 Å can be distinguished from a group of inordinately elongated distances > 2.5 Å, *all* of which are from structures with strained small rings in which the stronger bonds are to C, N or P and the Cr-S bond is probably pushed aside as a result of the greater polarizability of S. There is also a bimodal distribution within the main histogram peak that results in a cluster of bond distances from 2.38 to 2.42 Å, all from *transoid* Cr_2S_2 clusters involving a bridging η^2-S_2 linkage, which are likely to have some degree of π bonding; indeed these have a bond order of 1.2 by using Eqn. 1. A very distinct histogram peak is found between 2.33 – 2.37 Å for the η^2-DTDA's, that is structures of type **III** and **IV**, which are thus found to have Cr-S bond orders of 1.3 consistent with previously assigned π-bonding character to this class.[33-35] Another distinct group are the μ^3-S-CrFeCo clusters with *pseudo*-tetrahedron geometries, all found in the narrow range from 2.23 – 2.25 Å, corresponding to bond orders of 1.8 – 1.9.

It is now possible to confirm the Cr-S bond in **3** at 2.4908(11) Å as an almost ideal Cr-S single bond. Furthermore, the π-bonded structures of **6a,b** are found in a narrow distance range that is centred between the μ^3-S-CrFeCo clusters and the η^2-DTDA's. Their very similar Cr-S distances of 2.2987(14) in **6a** and 2.2965(11) Å in **6b** (mean = 2.298(3) Å) correspond to a bond order of 1.5, thus significantly higher than found in η^2-DTDA's.

There are far fewer data in the literature for Cr-N distances in $CpCr(CO)_x$ or $Cp*Cr(CO)_x$ derivatives (a histogram from 24 structures fitting these criteria is available in the SI as Figure S3). The majority of such structures are linear nitroxides with an average Cr-N bond distance of 1.75(4) Å. The remainder are 2-thiolatopyridines of the general type **VII**, in which the Cr-N distances are 2.06-2.10 Å.
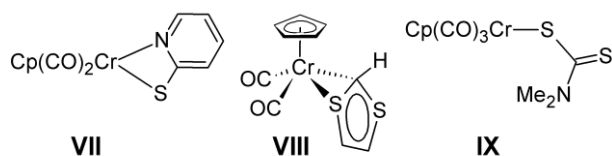
It is therefore necessary to consider the full range of chromium compounds with bonds to nitrogen to obtain a reasonable context. Searches of the CSD [release 1.16, November, 2013][70] show that the 2621 structures with Cr-N bonds display CrN distances with two maxima (Figure S4), the major peak is centred on 2.07 Å, and a much smaller peak is centred on 1.68 Å. A more selective analysis of the larger grouping indicates that the mean value for a Cr—N single bond is 2.06(7) Å; this is actually *shorter* than the estimate of 2.15(5) Å obtained from the updated covalent radii in Cordero *et al.*[71] A more selective analysis of the shorter distances is able to distinguish between genuine Cr≡N triple bonds in chromium

nitride complexes (Figure S5, mean Cr-N distance of 1.56(2) Å) and short CrN bonds in Cr=NR imido complexes at 1.64(2) Å (Figure S6). Using the mean single and triple bond distances just mentioned in a Pauling bond order analysis (Eqn. 1) yields a b value of 0.453 for nitrogen and assigns a bond order of 2.5 to the aforementioned Cr=NR imido complexes and 2.0 in metal nitroxides, which corresponds to the canonical structure CpCr=N=O. This analysis shows that the very similar Cr-N bond lengths in **6a** (2.100(4) Å) and **6b** (2.098(3) Å) are, perhaps surprisingly, somewhat elongated single bond lengths. To our knowledge, there is only one other structure in the literature with a comparable geometry, namely **VIII** (the entry with refcode RATROU in Table 1), in which a CpCr fragment is bound in a side-on manner through the C and S atom of the organic fragment, forming a three-membered Cr,S,C chelate ring; in this structure wherein the Cr—S bond length is comparable to that found in η^2-DTDAs, the Cr—C distance is also rather long at 2.144(3) Å, a value that is well within the single-bond range.[44]

The ligand bite angle (N-Cr-S) is very similar in both molecules (44.89(11)° in **6a** and 44.65(9)° in **6b**). The Cr-N-S and Cr-S-N angles are also similar (73.80(14)° and 61.31(13)° in **6a**; 73.94(12)° and 61.41(11)° in **6b**). In summary, the transformation accompanying the loss of one carbonyl group (step 2 in Scheme 2) that converts **3'** to **6** induces a change in Cr-S bond order from 1.0 to 1.5 and brings the N atom into bonding distance with a bond order of 0.9.

Computational results on 3.

In order to corroborate the bond order determinations from geometrical data and in the interest of describing the bonding in the unusual structures of **3** and **6a,b**, a detailed computational study using hybrid DFT methods has been undertaken at the B3PW91/6-311+G(2df,2p)//B3PW91/6-31G(2d,p) level of theory. Previous work in our laboratories has shown that the B3PW91 functional works extremely well at reproducing the metrics of thiazyl complexes of first-row transition metals.[33-35,73] The structure of complex **3** is unprecedented in the literature; there are *no* other known metal complexes derived from **2**, nor are there any known complexes of CpCr(CO)$_3$ in which a single S atom incorporated into a ring is coordinated to Cr. Indeed, in the N,N'-dimethylthiocarbamato-S derivative **IX** (structure refcode XUJGOY) the metal atom is found to be rigorously in the plane of the ligand and not coordinated perpendicularly to its well-developed π system.[49] The 3,5-diphenyl-λ^3-1-thia-2,4,6-triazinyl radical **2** thus demonstrates once again its remarkable properties in this metal complex. For context, we first recall that **2** is isolated in the solid state as the face-to-face diffusely-bonded dimer **2$_2$** with the property that whilst the strongest linkage is certainly between the two sulfur atoms (d_{SS} = 2.677(3) Å), or 26% < Σr_{vdW}, steric arguments would expect the geometry to be *transoid* unless there is also an interaction between the N and C atoms in the adjacent rings.[67] There are indeed short contacts between these atoms, ranging from

4% down to 1% < $\sum r_{vdW}$. Both the orientation and the cross-ring distances in 2_2 strongly resemble the well-known transannular interactions in the folded eight-membered ring structure of S_4N_4 (and the similar but less recognized such interaction in $S_4N_5^-$),[74,75] but the important distinction is that 2_2 is not constrained to such a *cis*-cofacial arrangement.

An interesting aspect of the structure of this self-dimerised species is that density functional theory in the gas phase is not able to reproduce such structures; in order to get a net binding energy it is necessary to use dispersion-corrected methods such as MO62X.[76-79] However, computational chemistry is very important to treat the structures and energetics of the monomers **1** and **2**, since these species cannot be studied directly. Similarly, the anionic form **2**⁻ is not known as the free ion, but was trapped by protonation to the imine. For consistency with data on the metal complexes, the geometries of the cation, radical and anion form of **2** were optimized at the B3PW91/6-31G(2d,p) level of theory and the bond distances within the C,N,S rings are listed in Table 2 along with experimental and computed values for complex **3**. These computational results strongly corroborate the prediction previously made from crystal structures of isolated **2**⁺, 2_2 and **2**H that the geometry of the thiatriazinyl ring fragment within **3** is intermediate between that of the neutral and anionic form; in fact, the *metrical* data suggest that the complex contains approximately **2**⁻⁰·⁵. This crude estimate is corroborated by analysis of the computed atomic charges in the geometry optimized structure of **3** which yields a net charge on the thiatriazinyl ring fragment of −0.30 *e* and on CpCr(CO)₃ of +0.30 *e*.

The computed geometry of **3** agrees quite well with that obtained from the crystal structure, save for a difference in rotation about the Cr—S bond (Figure 6, Table 2). To analyze this, we define the dihedral angle C21-Cr-S-N2 (see Fig. 1), linking the carbonyl group at the back of the complex, via Cr and S and down to the unique ring N atom; thus at 0°, the thiatriazinyl will be in the symmetrical eclipsed position with the ring substituents oriented down, i.e. on the side of the carbonyl groups. In the crystal structure, this dihedral angle is measured as −42.4(2)°; in the DFT optimized geometry this value is −54.8° (Figure 6); thus both are *very* far from the symmetrically eclipsed orientation. Further analysis is required to determine if this conformational preference is just steric in origin or due to some sort of orbital interaction.

Since this dihedral represents the main deviation between the experimental and computed structures, it was decided to analyze rotation of the structure about the Cr—S bond computationally. The results are depicted in Figure 7. Here the minima are the gauche conformations left (L) and right (R) of the symmetrical eclipsed (E) position. The staggered conformation (S) is 180° out of phase with eclipsed. The inflections marked by the asterisks are associated with a spontaneous change in the

orientation of the Cp group within ±4° of fully eclipsed. (Within this narrow range of angles, one point of the pentagon overlies the Cr-S bond; in the rest of the dihedral angle range, this point overlies the Cr-C21 bond as shown in Figure 6.) Since free rotation of the Cp ring is expected, these inflections may be ignored. The calculated barriers are thus ~13-14 kJ/mol. These values may be compared to rotational barriers in butane: 14.6 for the lower and 20.9 kJ/mol for the higher, fully eclipsed barrier.[80]

Figure 6 B3PW91/6-31G(d,p) calculated geometry in **3** (pipes) overlaid on that from the X-ray structure determination (displacement ellipsoids plot). The difference in C21-Cr-S1-N2 torsion angle stands out whereas the remainder of the structure shows excellent match between computation and experiment.
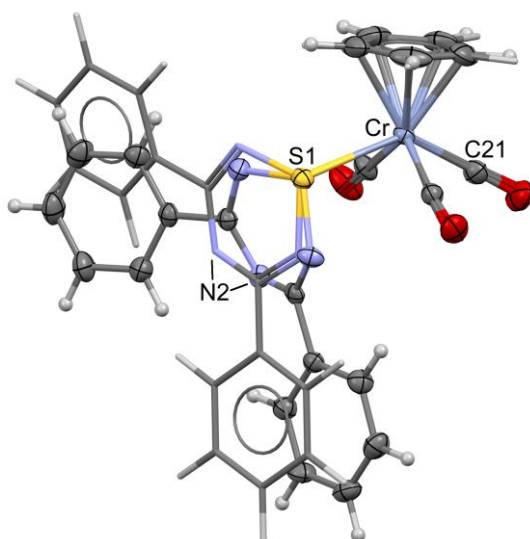
Figure 7 B3PW91/6-31G(d,p) calculated barrier height for rotation about the Cr–S bond in [CpCr(CO)₃(PhTTAPh)]. For the inflection points marked by *, see text.
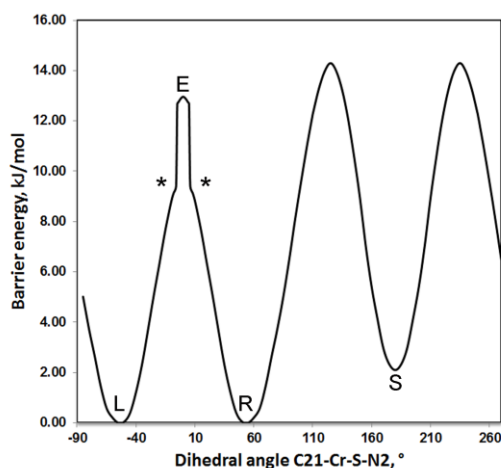
A careful analysis of the frontier molecular orbital (FMO) topologies and energies for computationally optimized **3** in comparison to those of the neutral fragments **1** and **2** (the latter computed at the geometries adopted in the complex) indicates that the bond between the two fragments is almost exclusively due to the interaction of their SOMOs. This is presented graphically in Figure 8, where the open-shell FMO energies are averages of the corresponding α and β wavefunction energies (a commonly encountered alternative, the restricted open-shell Hatree-Fock or ROHF, formalism results in much higher energies for the fragment SOMOs).[81] The topology of the bond involves an interaction between the π_4 SOMO of **2**, wherein the component S p_z orbital overlaps with a Cr $d_{x^2-y^2}$ orbital in the SOMO of **1**. The calculated binding energy between the fragments is 42.1 kJ·mol^{-1}. This value is considerably *less* than the stabilization of the two SOMOs (~92 kJ·mol^{-1}), and indeed the remaining filled MOs become significantly destabilized upon complex formation. Thus, despite the apparent stabilization of the four remaining filled d orbitals of the CpCr(CO)$_3$ unit, some eight thiatriazinyl ring orbitals are raised in energy considerably; that is, the proximity of the metal within the complex raises the energies of these orbitals. The net effect is a rather weak single bond through the occupied HOMO of the complex. There is therefore a strong agreement between the bonding analysis and the computed barriers showing facile bond rotation about a single bond.

Figure 8 Orbital interaction diagram showing the FMOs for the binding of [CpCr(CO)$_3$]$^{\bullet}$ and **2** to form **3** as determined from B3PW91/6-311+G(2df,2p)//B3PW91/6-31G(2d,p) hybrid DFT calculations.
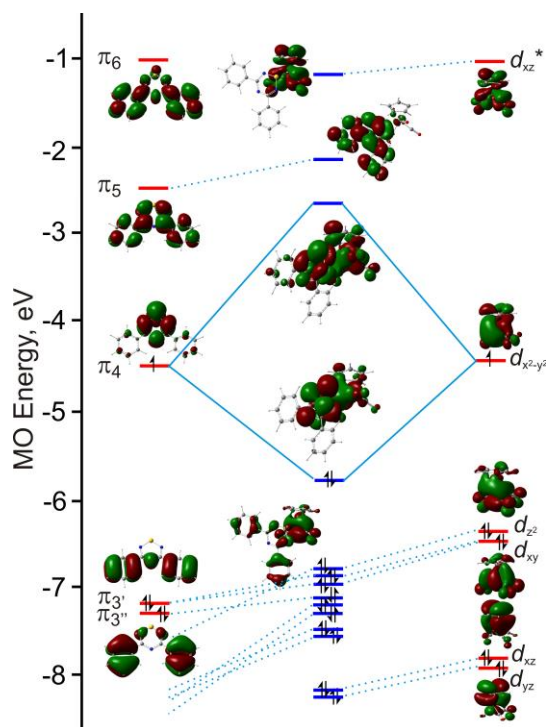
Computational results on 6a,b.

Computed geometries of **6a,b** at the B3PW91/6-31G(2d,p) hybrid DFT level agree well with those obtained from the solid-state structure determinations (Tables 3 and 4). As mentioned above, both crystal structures are found in the *exo* conformation (defined w.r.t. the relative orientations of the TTA and Cp rings at chromium); this contrasts with 1,2,3,5-dithiadiazolyl complexes **III** and **IV** where different substituents on the aryl groups lead to either *exo* or *endo* conformations. Therefore the geometries of **6a,b** were computed as putative *exo* and *endo* isomers and optimized structures are obtained for both geometric isomers (see Figure 9 for resulting structures), each with very reasonable geometries and forming stable minima (no imaginary frequencies). The energies of the two isomers at the B3PW91/6-311+G(2df,2p) level of theory are only marginally different, with **6a** preferentially *exo* and **6b** *endo*, with computed differences of less than 1 kJ mol^{-1} that are smaller than the estimated precision of such calculations. There is thus every reason to expect that under suitable crystallization conditions the *endo* isomers of **6** could also be isolated if thiatriazinyls with a greater diversity of aryl group substituents were employed to make such complexes.

Figure 9 B3PW91/6-31G(2d,p) calculated geometries in **6a**, in (a) *exo* and (b) *endo* geometric isomers.
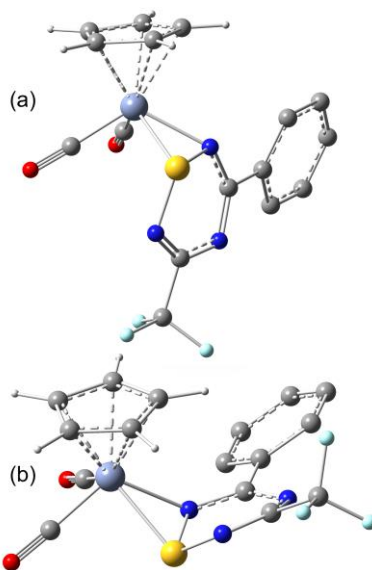
The metrical data comparing both the computed and experimental data for **5a** and **6a** are compiled in Table 3, and similar results for **5b** and **6b** can be found in Table 4. For the two metal complexes, there is again excellent agreement between the DFT-computed and the X-ray data and they are also quite similar to each other. Thus, the important Cr–S bond distances computed for **6a,b** at 2.303 and 2.302 agree closely to the measured values of 2.2965(11) and 2.2987(14) Å, respectively. Similarly good

agreement can be found for all the distances and even the angles agree very well. These data tables also compile the geometrical data calculated for the *endo* isomers of **6a,b**, both of which are predicted to have marginally longer Cr–S bond lengths.

It is also possible to compare the distances in **6a,b** within the thiatriazinyl ring with the values computed for free **5a,b**$^-$ anions and **5a,b** radicals; most of such distances in **6a,b** are found to be intermediate between those of ligand anion and ligand radical. However, due to the lower symmetry (compared to **2**), it seems more reliable to turn once again to the computed atomic charges to establish the thiatriazinyl charge states in these complexes. These yield a net charge on the thiatriazinyl ring fragment in **6a** of −0.22 *e* with CpCr(CO)$_2$ at +0.22 *e*, while for **6b**, the ring is −0.21 *e* with CpCr(CO)$_2$ at +0.21 *e*. Though quite close to the values calculated for **3** (see above), the fact that the negative charge concentration on the thiatriazinyls (the entire moiety including the trifluoromethyl group) is lower despite the strongly electron withdrawing CF$_3$ substituents, probably indicates stronger "back-bonding" to the metal in **6a,b**.

Calculations were also performed on the component fragments as open shell species, that is monomeric **5a,b** and CpCr(CO)$_2$$^\bullet$ radicals (using the geometries as found in the complexes), and from the difference between energies of the sums of the components and the optimized complexes (without relaxation) the adiabatic binding energies are found to be −195 kJ mol^{-1} for **6a** and -193 kJ mol^{-1} for **6b**. Thus, the binding energies of the η^2-thiatriazinyls **5a,b** to CpCr(CO)$_2$ are about four times larger than that calculated for the η^1-thiatriazinyl **2** to CpCr(CO)$_3$.

A consideration of the FMOs of the fragments and the complex that were used for the binding energy determinations was undertaken for **6a** and the results are shown in Figure 10 (here too the fragment FMOs are averages of α and β wavefunction energies).[81] By comparison with Figure 8, it is immediately apparent that the binding in **6a** is considerably stronger than in **3**. The greatest stabilization occurs for the CpCr(CO)$_2$ d_{xy} orbital which by interaction with the π^4 SOMO of **5a** is lowered in energy by ~2.5 eV and forms the most important bonding FMO of **6a**, an orbital that is sufficiently stabilized to become the third-highest filled level in the complex. In contrast, the d_{z^2} HOMO is barely stabilized upon binding, while $d_{x^2-y^2}$ interacts less strongly with the π orbitals of **5a**. There is a considerable amount of re-hybridization of these ring π orbitals upon binding due to the lowered symmetry, so that all three metal "t_{2g}-like" d orbitals interact with somewhat similar "pseudo-π" orbitals. The combined strong stabilization of d_{xy} and the weaker stabilizations of d_{z^2} and $d_{x^2-y^2}$ account for the majority of the binding interaction and are consistent with the measured Cr–S bond order of 1.5 in **6a,b**. The higher bond order of these complexes compared to the dithiadiazolyl complexes of type **III** and **IV** is also reflected in the

greater stabilization of d_{xy} in the interaction with the ring π orbitals (see supporting information to Ref. 34) and the consequent reversal in the sequence of the HOMOs of the complexes from $d_{xy} > d_{z^2} > d_{x^2-y^2}$ to $d_{z^2} > d_{x^2-y^2} > d_{xy}$.

Figure 10 Orbital interaction diagram for the binding of $[CpCr(CO)_2]^{\bullet}$ and **5a** to form **6a** as determined from B3PW91/6-311+G(2df,2p)//B3PW91/6-31G(2d,p) hybrid DFT calculations.

Redox compatibility.

The redox potentials for the monomeric radical species involved in the reactions leading to **3** and **6a,b** are known from a number of careful studies in the literature.[62,63,82] These provide insight into the aforementioned mild interactions that seem to occur between $[CpCr(CO)_{2,3}]^{\bullet}$ and thiatriazinyls. A representation comparing the mid-point potentials (corresponding in thermodynamic terms to equilibrium concentrations of each of the reactive species) is shown in Figure 11. This demonstrates visually that the redox potentials of at least $[CpCr(CO)_3]^{\bullet}$,[63] **2** [82] and **5a,b** [62] are compatible when each species is present as a neutral radical. This is likely a reason that insertion reactions (involving oxidative addition) do not operate under the mild reaction conditions employed here. The data also show that the CF_3-substituted radicals **5a,b** are more oxidizing than is **2**; whether this is a driving force for the

apparently easier displacement of the third carbonyl ligand in the conversion of **3'** to **6** is not clear, in part because the redox potentials of [CpCr(CO)$_2$]$^\bullet$ are not known.

Figure 11 Representation of the redox compatibilities for **2**, **5a,b** and monomeric [CpCr(CO)$_3$]$^\bullet$. Vertical lines represent the formal potentials between neighbouring species, in volts *vs*. the Fc$^{+/0}$ redox couple, as determined in CH$_3$CN/[^{n}Bu$_4$N][PF$_6$] solutions.

Conclusions

The suppression of oxidative addition when thiatriazinyl radicals and organometallic [CpCr(CO)$_3$]$^\bullet$ radicals interact under mild conditions has enabled the isolation and structure determination of the second type of ring π complex containing thiazyl linkages, after the earlier discovery of η^2-DTDA complexes with the same metal fragments. Likely this success can be attributed to weak redox reactions as a result of very compatible ligand and metal potential ranges.

In **3**, the Cr—S bond has the metric expected for a single bond, there is no obvious back-bonding interaction between the thriatriazinyl **2** and the metal as determined by an FMO analysis, and the computed rotational barrier fits what is expected for rotation about a single bond. Thus, even though the orientation of the metal is distinctly perpendicular to that of the ring, it is after all best described as a σ-type bond that forms between two π moieties. This feature recalls the dichotomy encountered in cyclic structures which enable π-delocalised NSN moieties to approach perpendicularly to form a transannular σ bond between the two fragments using rehybridised π orbitals from two NSN units.[69] In **3**, one of these NSN units can evidently be replaced by a CpCr(CO)$_3$ $d_{x^2-y^2}$ orbital.

However, when fluorinated thiatriazinyl ring π systems, namely **5a,b**, interact more strongly with CpCr(CO)$_3$, resulting in the displacement of one equivalent of carbon monoxide, a classical π interaction occurs in the resulting η^2 complexes **6a,b**. The bonding involves perpendicular *p* orbitals on adjacent S and N atoms interacting with the full array of the "t_{2g}-like" *d* orbitals of the organometallic fragment. These results, as obtained from bonding analyses based on DFT calculations, are consistent with the Cr— S bond orders determined in this work for both **3** (B.O. = 1) and **6** (B.O. = 1.5), using the extensive data

accumulated during over 30 years of study of CpCr complexes with a wide variety of sulfur-containing ligands. Further work in our laboratories will continue to expand the search for thiazyl radicals that might form π complexes through interaction with CpCr(CO)$_3$$^•$ and similar organometallic radicals. In this search, we hope also to eventually isolate *endo* isomers of **6**.

Experimental

General methods.

All manipulations were carried out either under an argon atmosphere using standard Schlenk techniques or under an argon atmosphere in an MBraun Labmaster 130 glove box. ^{1}H NMR spectra were recorded using a Bruker ACF 300 MHz FT NMR spectrometer, with chemical shifts referenced to residual solvent peaks in the respective deuterated solvents. IR spectra were measured in the range 4000-400 cm^{-1} in KBr pellets on a Bio-Rad FTS165 FTIR spectrophotometer. Mass spectra were obtained on Finnigan-MAT 95XL-T (FAB) or Finnigan-MAT VG Micromass 7035 (EI) spectrometers. Elemental analyses were performed by the National University of Singapore microanalytical laboratory. All solvents used were of analytical grade. They were dried and freshly distilled before use, according to standard procedures. Silica gel (Merck Kieselgel 60, 230-400 mesh) was dried at 140 °C overnight before chromatographic use. [CpCr(CO)$_3$]$_2$ (**1**) was prepared according to literature procedures from chromium hexacarbonyl (98% purity from Fluka).[65] Thiatriazinyls **2** and **5a,b** were prepared by published procedures and purified by vacuum sublimation in a three-zone tube furnace.[62,66,67]

Synthesis.

Reaction of [CpCr(CO)$_3$]$_2$ with [3,5-Ph-C$_2$N$_3$S]$_2$

A deep green mixture of [CpCr(CO)$_3$]$_2$ (**1**) (8 mg, 0.02 mmol) and [3,5-Ph$_2$-C$_2$N$_3$S]$_2$ (**3**) (10 mg, 0.02 mmol) in toluene (12 mL) was stirred at ambient temperature for 4 h, at which point the ^{1}H NMR spectra of the reaction mixture indicated a 4:1 molar ratio of CpCr(CO)$_3$SN$_3$C$_2$Ph$_2$ (**3**) and [CpCr(CO)$_2$]$_2$S (**4**). The brownish-green product mixture was filtered through a plug of cotton wool in a disposable pipette to remove any insoluble impurities. Concentration of the filtrate *in vacuo* to ca. 3 mL, followed by addition of n-hexane (6 mL) and subsequent cooling at -29 °C for one day, gave dark red microcrystalline solids of CpCr(CO)$_3$SN$_3$C$_2$Ph$_2$, **3**, (ca. 10 mg, 0.02 mmol, 55% yield). The ^{1}H NMR spectrum of the mother liquor in benzene-d$_6$ showed that only [CpCr(CO)$_2$]$_2$S, **4**, remained behind. Diffraction-quality crystals of **3** were obtained from a toluene solution layered with hexane at -29°C after 2 days.

Anal. Found: C, 58.27; H, 3.50; N, 9.39; S, 7.21%. Calc. for C$_{22}$H$_{15}$CrO$_3$SN$_3$·0.15C$_7$H$_8$: C, 58.27; H, 3.33; N, 9.27; S, 7.07%. ^{1}H NMR (300 MHz, 300K, C$_6$D$_6$): δ(Cp) 4.29 (s, 5H); δ(C$_6$H$_5$) 8.49 (m, 10H). IR (KBr, cm^{-1}): ν(C≡O) 1955vs, 1874vs; ν(others) 1586w, 1529s, 1484w, 1455m, 1424m, 1321m, 1292w, 1265m, 1161w,

1135vw, 1064vw, 1025w, 943vw, 816w, 794vw, 754w, 720m, 687w, 632vw, 577vw, 541vw, 475vw. FAB$^+$-MS: m/z 426 [M-CO+1]$^+$, 369 [M-2CO]$^+$, 253 [SN$_3$C$_2$Ph$_2$+1]$^+$, 149 [M-3CO-N$_3$C$_2$Ph$_2$]$^+$.

Reaction of [CpCr(CO)$_3$]$_2$ (1) with [3-Ph-5-CF$_3$-C$_2$N$_3$S]$_2$ (5a)

A dark green solution of [CpCr(CO)$_3$]$_2$ (**1**) (5 mg, 0.01 mmol) in 2 mL of toluene was added to a solution of [3-Ph-5-CF$_3$-C$_2$N$_3$S]$_2$ (**5a**) (6 mg, 0.01 mmol) in 1 mL toluene by layering in a test tube, and the resultant dark red mixture immediately kept at -29 °C. After 3 days, the layers have diffused but no crystals were formed. Hence the reaction mixture was concentrated *in vacuo* to *ca.* 2 mL, followed by addition of n-hexane (4 mL). Subsequent cooling at -29 °C for 1 day yielded two crops of dark red microcrystalline solids of CpCr(CO)$_2$SN$_3$C$_2$PhCF$_3$ (**6a**) (*ca.* 4 mg, 0.007 mmol, 30% combined yield). Diffraction quality crystals of **6a** were obtained from toluene layered with n-hexane at −29 °C after 3 days.

^{1}H NMR (300 MHz, 300K, C$_6$D$_6$): δ(Cp) 4.24 (s, 5H); δ(C$_6$H$_5$) 8.54 (m, 3H); δ(C$_6$H$_5$) 8.44 (m, 2H). IR (KBr, cm^{-1}): ν(C≡O) 1965vs, 1907vs; ν(others) 1630m, 1563m, 1396m, 1273w, 1202m, 1142m, 1064m, 825w, 694m, 536w, 471w. FAB$^+$-MS: m/z 361 [M-2CO]$^+$, 77 [Ph]$^+$. FAB$^-$-MS: m/z 244 [SN$_3$C$_2$PhCF$_3$]$^-$, 164 [M-2CON$_3$C$_2$PhCF$_3$]$^-$.

Reaction of [CpCr(CO)$_3$]$_2$ with [4-MeOC$_6$H$_4$-5-CF$_3$-C$_2$N$_3$S]$_2$

A deep green mixture of [CpCr(CO)$_3$]$_2$ (**1**) (9 mg, 0.02 mmol) and [4-MeOC$_6$H$_4$-5-CF$_3$-C$_2$N$_3$S]$_2$ (**5b**) (11 mg, 0.02 mmol) in toluene (12 mL) was stirred at ambient temperature for 4 h. The ^{1}H NMR spectrum of the reaction mixture showed that the reaction was complete. The resultant brownish red product mixture was filtered through a plug of cotton wool in a disposable pipette to remove any insoluble impurities. Concentration of the filtrate *in vacuo* to *ca.* 3 mL, followed by addition of n-hexane (6 mL) and subsequent cooling at −29 °C for 1 day, gave 2 crops of dark red microcrystalline solids of CpCr(CO)$_2$SN$_3$(CCF$_3$)(C$_6$H$_4$OCH$_3$) (**6b**) (*ca.* 4 mg, 0.009 mmol, 20% combined yield). Diffraction-quality crystals of **6b** were obtained from toluene layered with n-hexane at −29 °C after 2 days.

Anal. Found: C, 46.06; H, 2.51; N, 9.33; S, 6.85%. Calc. for C$_{17}$H$_{12}$CrF$_3$N$_3$O$_3$S: C, 45.64; H, 2.70; N, 9.39; S, 7.17%. ^{1}H NMR (300 MHz, 300K, C$_6$D$_6$): δ(Cp) 4.22 (s, 5H); δ(C$_6$H$_4$) 8.23 (d, 2H), 6.72 (d, 2H), δ(OCH$_3$) 3.18 (s, 3H). IR (KBr, cm^{-1}): ν(C≡O) 1957vs, 1873vs; ν(others) 1599m, 1550m, 1426m, 1376s, 1257s, 1204m, 1166m, 1066w, 1024w, 764vw, 580vm, 472vw. FAB$^+$-MS: m/z 448 [M+1]$^+$, 391 [M-2CO]$^+$.

X-ray crystallography.

X-ray intensity data on crystals of **3** and **6a,b** were collected on a Siemens SMART diffractometer, equipped with a CCD detector, using Mo(Kα) radiation (λ = 0.71073 Å). The data were corrected for Lorentz and polarization effects with the SMART suite of programs and for adsorption effects with

SADABS.[83] Structure solution and refinement were carried out with the SHELXTL suite of programs.[84] The structures were solved by direct methods to locate the heavy atoms, followed by difference maps for the non-hydrogen atoms. Hydrogen atoms attached to carbon were placed in calculated positions with C–H = 0.95 Å and U_{iso} = 1.2U_{eq}(C) for the purpose of model refinement. Crystal and experimental parameters are compiled in Table 5, and selected interatomic distances are available in Tables 2-4. Electronic structures in CIF format are provided with the supporting information.

Computation.

Previous work in our laboratories has shown that the B3PW91 functional works extremely well at reproducing the metrics of thiazyl complexes of first-row transition metal organometallics [33-35,73] so this method is also adopted in this study. For consistency, all the calculations were performed with the same functional, including the ligand geometries. Geometry optimizations were undertaken using a medium sized (6-31G(2d,p)) Gaussian basis set and the determination of local minima confirmed by the absence of imaginary frequencies in all cases. Final energy calculations for determination of binding energies employ the large triple ζ 6-311+G(2df,2p) basis set. Open and closed shell species employed unrestricted and restricted methods, respectively. All calculations were performed using Gaussian03W installed on an eight-coprocessor personal computer; the barrier height for rotation about the Cr–S bond made use of the "scan" routine within the Gaussian program suite.[85] Cartesian coordinates of computed structures are provided in the supporting information in electronic (CIF) and print formats.

Supplementary material

Supplementary material is available with the article through the journal Web site at http://nrcresearchpress.com/doi/suppl/...... Structure depositions: **3**, CCDC 614495; **6a**, CCDC 614496; **6b**, CCDC 1005252 contain the supplementary crystallographic data for this paper. These data can be obtained, free of charge, via http://www.ccdc.cam.ac.uk/products/csd/request/ (or from the Cambridge Crystallographic Data Centre, 12 Union Road, Cambridge CB2 1EZ, U.K. (Fax: 44-1223-336033 or e-mail: deposit@ccdc.cam.ac.uk)).

Acknowledgements

References

(1)   Matsuo, Y.; Maruyama, M. *Chem. Commun.* **2012**, *48*, 9334.

(2)   Fischer, R. C.; Power, P. P. *Chem. Rev.* **2010**, *110*, 3877.

(3)   Jones, C. *Coord. Chem. Rev.* **2010**, *254*, 1273.

(4)   Kira, M. *Chem. Commun.* **2010**, 2893.

(5)   Mizuhata, Y.; Sasamori, T.; Tokitoh, N. *Chem. Rev.* **2009**, *109*, 3479.

(6)   Wang, Y.; Robinson, G. H. *Chem. Commun.* **2009**, 5201.

(7)   Scheschkewitz, D. *Chem. Eur. J.* **2009**, *15*, 2476.

(8)   Tokitoh, N.; Sasamori, T. *Dalton Trans.* **2008**, 1395.

(9)   Ottoson, H.; Eklöf, A. M. *Coord. Chem. Rev.* **2008**, *252*, 1287.

(10)   Lee, V. Y.; Sekiguchi, A. *Acc. Chem. Res.* **2007**, *40*, 410.

(11)   Rivard, E; Power, P. P. *Inorg. Chem.* **2007**, *46*, 10047.

(12)   Wang, Y.; Robinson, G. H. *Organometallics* **2007**, *26*, 2.

(13)   Power, P. P. *Organometallics* **2007**, *26*, 4362.

(14)   Ottoson, H.; Steel, P. G. *Chem. Eur. J.* **2006**, *12*, 1576.

(15)   Sekiguchi, A.; Ichinohe, M.; Kinjo, R. *Bull. Chem.Soc. Jpn.* **2006**, *79*, 825.

(16)   Kira, M.; Iwamoto, T. *Adv. Organomet.Chem.* **2006**, *54*, 73.

(17)   Power, P. P. *Chem. Rev.* **1999**, *99*, 3463.

(18)   Maslowsky, E. Jr. *Coord. Chem. Rev.* **2011**, *255*, 2746.

(19)   Turbervill, R. S. P.; Goicoechea, J. M. *Inorg. Chem.* **2013**, *52*, 5527.

(20)   Yuan, Y.; Cheng, L. *J. Chem. Phys.* **2013**, *138*, article 024301.

(21)   Knapp, C. M.; Westcott, B. H.; Raybould, M. A. C.; McGrady, J. E.; Goicoechea, J. M. *Angew. Chem. Int. Ed.* **2012**, *51*, 9097.

(22)   Ly, H. V.; Moilanen, J. Tuononen, H. M.; Parvez, M.; Roesler, R. *Chem. Commun.* **2011**, *47*, 8391.

(23)   Wolf, R.; Ehlers, A. W.; Khusniyarov, M. M.; Hartl, F.; de Bruin, B.; Long, G. J.; Grandjean, F.; Schappacher, F. M.; Pöttgen, R.; Slootweg, J. C.; Lutz, M.; Spek, A. L.; Lammertsma, K. *Chem. Eur. J.* **2010**, *16*, 14322.

(24)   Miao, C-Q.; Chen, Q.; Guo, J-C.; Li, S-D. *Sci. China, Ser. B: Chem.* **2010**, *53*, 940.

(25)   Landorf, C. W.; Haley, M. M. *Angew. Chem. Int. Ed.* **2006**, *45*, 3914.

(26)   Chen, J.; Jia, G. *Coord. Chem. Rev.* **2013**, *257*, 2491-2521.

(27)   Shi, C.; Guo, T.; Poon, K. C.; Lin, X; Jia, G. *Dalton Trans.* **2011**, 11315.

(28) Boeré, R. T.; Roemmele, T. L. Chalcogen–Nitrogen Radicals. In: Reedijk, J,; Poeppelmeier, K. Eds. *Comprehensive Inorganic Chemistry: From Elements to Applications,* II, Elsevier: Oxford, 2013. Vol 1, p. 375.

(29) Preuss, K. E. *Dalton Trans.* **2007**, 2357.

(30) Banister, A. J.; May, I.; Rawson, J. M.; Smith, J. N. B. *J. Organomet. Chem.* **1998**, *550*, 241.

(31) Roesky, H. W.; Gries, T.; Hofmann, H.; Schimkowiak, J.; Jones, P. G.; Meyer-Bäse, K.; Sheldrick, G. M. *Chem. Ber.* **1986**, *119*, 366.

(32) Boeré, R. T.; Moock, K. H.; Klassen, V.; Weaver, J.; Lentz, D.; Michael-Schulz, H. *Can. J. Chem.* **1995**,*73*, 1444.

(33) Lau, H. F.; Ang, P. C. Y.; Ng, V. W. L.; Kuan, S. L.; Goh, L. Y.; Borisov, A. S.; Hazendonk, P.; Roemmele, T. L.; Boeré, R. T.; Webster, R. D. *Inorg. Chem.* **2008**, *47*, 632.

(34) Lau, H. F.; Ng, V. W. L.; Koh, L. L.; Tan, G. K.; Goh, L. Y.; Roemmele, T. L.; Seagrave, S. D.; Boeré, R. T. *Angew. Chem. Int. Ed. Engl.* **2006**, *45*, 4498.

(35) Boeré, R. T.; Goh, L. Y.; Ang, C. Y.; Kuan, S. L.; Lau, H. F.; Ng, V. W. L.; Roemmele, T. L.; Seagrave, S. D. *J. Organomet. Chem.* **2007**, *692*, 2697.

(36) Ang, C. Y.; Boeré, R. T.; Goh, L. Y.; Koh, L. L.; Kuan, S. L.; Tan, G. K.; Yu, X. *Chem. Comm*. **2006**, 4735.

(37) Hankin, D. M.; Danopoulos, A. A.; Wilkinson, G.; Sweet, T. K. N.; Hursthouse, M. B. *J. Chem. Soc., Dalton Trans.* **1996**, 1309.

(38) Hankin, D. M.; Danopoulos, A. A.; Wilkinson, G.; Sweet, T. K. N.; Hursthouse, M. B. *J. Chem. Soc., Dalton Trans.* **1995**, 1059.

(39) Hankin, D. M.; Danopoulos, A. A.; Wilkinson, G.; Sweet, T. K. N.; Hursthouse, M. B. *J. Chem. Soc., Dalton Trans.* **1996**, 4063.

(40) Goh, L. Y.; Hambley, T. W.; Robertson, G. B. *Chem. Commun.* **1983***, 1458.

(41) Shen, J-Y.; Hu, Q-M. *Sci. China, Ser. B: Chem.* **1993**, *36*, 1281.

(42) Greenhough, T. J.; Kolthammer, B. W. S.; Legzdins, P.; Trotter J. *Inorg. Chem,* **1979**, *18*, 3542.

(43) Song, L-C.; Cheng, H-W.; Hu, Q-M.; Wang, Z. *J. Organomet. Chem.* **2004**, *689*, 139.

(44) Ng, V. W-L.; Kuan, S-L.; Weng, Z.; Leong, W. K.; Vittal, J. J.; Koh, L. L.; Tan, G-K.; Goh, L. Y. *J. Organomet. Chem.* **2005**, *690*, 2323.

(45) Herrmann, W. A.; Rohrmann, J.; Noth, H.; Narula, C. K.; Bernal, I.; Draux, M. *J. Organomet. Chem.* **1985**, *284***,** 189.

(46) Goh, L. Y.; Hambley, T. W.; Robertson, G. B. *Organometallics* **1987**, *6*, 1051.

(47) Ng, V. W-L.; Weng, Z.; Vittal, J. J.; Koh, L. L.; Tan, G. K.; Goh, L. Y. *J. Organomet. Chem.* **2005**, *690*, 1157.

(48) Wong, R. C. S.; Ooi, M. L.; Chee, C. F.; Tan G. H. *Inorg. Chim. Acta.,* **2005**, *358*, 1269.

(49) Goh, L. Y.; Weng, Z.; Leong, W. K.; Leung, P. H. *Organometallics* **2002**, *21*, 4398.

(50) Goh, L. Y.; Tay, M. S.; Mak, T. C. W.; Wang, R-J. *Organometallics* **1992**, *11*, 1711.

(51) Sukcharoenphon, K.; Moran, D.; Schleyer, P. v. R.; McDonough, J .E.; Abboud, K. A.; Hoff, C. D. *Inorg. Chem.* **2003**, *42*, 8494.

(52) Pasynskii, A. A.; Skabitskii, I. V.; Torubaev, Yu. V.; Dobrokhotova, Zh. V.; Krasil'nikov E. V. *Russ. J. Inorg. Chem.* **2005**, *50*, 1293.

(53) Ng, V. W-L.; Weng, Z.; Lip, L. K.; Tan, G-K.; Goh, L. Y. *J. Organomet. Chem.* **2004**, *689*, 3210.

(54) Shin, R. Y. C.; Ng, V. W. L.; Koh, L. L.; Tan, G. K.; Goh, L. Y.; Webster, R. D. *Organometallics* **2007**, *26*, 4555.

(55) McDonough, J. E.; Weir, J. J.; Carlson, M. J.; Hoff, C. D.; Kryatova, O. P.; Rybak-Akimova, E. V.; Clough, C. R.; Cummins, C. C. *Inorg. Chem.* **2005**, *44*, 3127.

(56) Goh, L. Y.; Weng, Z.; Leong, W. K.; Haiduc, I.; Lo, K. M.; Wong, R. C. S. *J. Organomet. Chem.* **2001**, *631*, 67.

(57) Weng, Z.; Leong, W. K.; Vittal, J. J.; Goh, L. Y. *Organometallics* **2003**, *22*, 1645.

(58) Goh, L. Y.; Chen, W.; Wong, R. C. S. *Angew. Chem., Int. Ed.* **1993**, *32*, 1728.

(59) Goh, L. Y.; Weng, Z.; Leong, W. K.; Vittal, J. J. *J. Am. Chem. Soc.* **2002**, *124*, 8804.

(60) Goh, L. Y.; Weng, Z.; Leong, W. K.; Vittal, J. J.; Haiduc, I. *Organometallics* **2002***, 21*, 5287.

(61) Scheer, M.; Umbarkar, S. B.; Chatterjee, S.; Trivedi, R.; Mathur, P. *Angew. Chem., Int. Ed.* **2001***, 40*, 376.

(62) Boeré, R. T.; Roemmele, T. L.; Yu, X. *Inorg. Chem.* **2011**, *50*, 5123.

(63) Barbini, D. C.; Tanner, P. S.; Francone, T. D.; Furst, K. B.; Jones, W. E. *Inorg. Chem*. **1996**, *35*, 4017.

(64) Boeré, R. T.; Roemmele, T. L. *Phos. Sulf. Silicon* **2004**, *179*, 875.

(65) Manning, A. R.; Hackett, P.; Birdwhistell, R.; Soye, P. *Inorg. Synth.* **1990**, *28*, 148.

(66) Cordes, A. W.; Hayes, P. J.; Josephy, P. D.; Koenig, H.; Oakley, R. T.; Pennington, W. T. *Chem. Commun.* **1984**, 1021.

(67) Hayes, P. J.; Oakley, R. T.; Cordes, A. W.; Pennington, W. T. *J. Am. Chem. Soc.* **1985**, *107*, 1346-1351.

(68) Boeré, R. T.; Cordes, A. W.; Hayes, P. J.; Oakley, R. T.; Reed, R. W.; Pennington, W. T. *Inorg. Chem.* **1986**, *25*, 2445.

(69)   Oakley, R. T. *Prog. Inorg. Chem.* **1988**, *36*, 299.

(70)   Allen, F. H. *Acta Cryst*. **2002**, B*58*, 380.

(71)   Cordero, B.; Gómez, V.; Platero-Prats, A. E.; Revés, M.; Echeverría, J.; Cremades, E.; Barragán F.; Alvarez, S. *Dalton Trans.* **2008**, 2832.

(72)   Lendvay, G. *J. Mol. Struct. (Theochem)* **2000**, *501-502*, 389.

(73)   Boeré, R. T. *Cryst. Growth Des.* **2014**, 814.

(74)   Moock, K. H.; Wong, K. M.; Boeré, R. T. *Dalton Trans.* **2011**, *40*, 11599.

(75)   Boeré, R. T.; Roemmele, T. L.; Krall, M. K. *Molecules* **2014**, *19*, 1956.

(76)   Beneberu, H. Z.; Tian, Y-H.; Kertesz, M. *Phys. Chem. Chem. Phys.* **2012**, *14*, 10713.

(77)   Kolb, B.; Kertesz, M.; Thonhauser, T. *J. Chem. Phys. A* **2013**, *117*, 3642.

(78)   Boeré, R. T.; Roemmele, T. L. *Manuscript in preparation.*

(79)   Cui, Z-H.; Lischka, H.; Beneberu, H. Z.; Kertesz, M. *J. Am. Chem. Soc.* **2014**, *136*, 5539.

(80)   Anslyn, Eric; Dennis Dougherty (2006). *Modern Physical Organic Chemistry*. University Science. p. 95.

(81)   Jensen, Frank (2007). *Computational Chemistry*. Willey, p. 99ff.

(82)   Boeré, R. T.; Roemmele, T. L. *Coord. Chem. Rev*. **2000**, *210*, 369.

(83)   Bruker **2008**. APEX2, SAINT-Plus and SADABS. Bruker AXS Inc., Madison, Wisconsin, USA.

(84)   Sheldrick, G. M. *Acta Cryst.* **2008**, A*64*, 112.

(85)   Gaussian 03W, Revision E.01, Frisch, M. J.; Trucks, G. W.; Schlegel, H. B.; Scuseria, G. E.; Robb, M. A.; Cheeseman, J. R.; Montgomery, Jr., J. A.; Vreven, T.; Kudin, K. N.; Burant, J. C.; Millam, J. M.; Iyengar, S. S.; Tomasi, J.; Barone, V.; Mennucci, B.; Cossi, M.; Scalmani, G.; Rega, N.; Petersson, G. A.; Nakatsuji, H.; Hada, M.; Ehara, M.; Toyota, K.; Fukuda, R.; Hasegawa, J.; Ishida, M.; Nakajima, T.; Honda, Y.; Kitao, O.; Nakai, H.; Klene, M.; Li, X.; Knox, J. E.; Hratchian, H. P.; Cross, J. B.; Bakken, V.; Adamo, C.; Jaramillo, J.; Gomperts, R.; Stratmann, R. E.; Yazyev, O.; Austin, A. J.; Cammi, R.; Pomelli, C.; Ochterski, J. W.; Ayala, P. Y.; Morokuma, K.; Voth, G. A.; Salvador, P.; Dannenberg, J. J.; Zakrzewski, V. G.; Dapprich, S.; Daniels, A. D.; Strain, M. C.; Farkas, O.; Malick, D. K.; Rabuck, A. D.; Raghavachari, K.; Foresman, J. B.; Ortiz, J. V.; Cui, Q.; Baboul, A. G.; Clifford, S.; Cioslowski, J.; Stefanov, B. B.; Liu, G.; Liashenko, A.; Piskorz, P.; Komaromi, I.; Martin, R. L.; Fox, D. J.; Keith, T.; Al-Laham, M. A.; Peng, C. Y.; Nanayakkara, A.; Challacombe, M.; Gill, P. M. W.; Johnson, B.; Chen, W.; Wong, M. W.; Gonzalez, C.; and Pople, J. A.; Gaussian, Inc., Wallingford CT, 2004.

Table 1. Compilation of Cr—S bond distances in all crystal structures of CpCr(CO)$_x$S derivatives.

Metal group[a]	Cr—S, Å	Bond order	Class[b]	Descriptor[b]	Refcode[c]	Lit. ref.
CpCr(CO)$_2$	2.0692(7)	3.0	1	Lin. br. S$_1$	SCPDCC01	40
Cp'Cr(CO)$_2$	2.071(3)	3.0	1	Lin. br. S$_1$	YODZAS	41
CpCr(CO)$_2$	2.0713(2)	3.0	1	Lin. br. S$_1$	SCPDCC	42
CpCr(CO)$_2$	2.0717(7)	3.0	1	Lin. br. S$_1$	SCPDCC01	40
CpCr(CO)$_2$	2.0721(2)	3.0	1	Lin. br. S$_1$	SCPDCC	42
Cp'Cr(CO)$_2$	2.074(3)	2.9	1	Lin. br. S$_1$	YODZAS	41
CpCr(CO)$_2$	2.0759(7)	2.9	1	Lin. br. S$_1$	SCPDCC01	40
CpCr(CO)$_2$	2.0760(2)	2.9	1	Lin. br. S$_1$	SCPDCC	42
CpCr(CO)$_2$	2.0767(7)	2.9	1	Lin. br. S$_1$	SCPDCC01	40
CpCr(CO)$_2$	2.0771(2)	2.9	1	Lin. br. S$_1$	SCPDCC	42
CpCr(CO)$_2$	2.230(2)	1.9	2	Sμ^3-CrFeCo cluster	IRIJAU	43
CpCr(CO)$_2$	2.232(2)	1.8	2	Sμ^3-CrFeCo cluster	IRIJAU	43
CpCr(CO)$_2$	2.241(2)	1.8	2	Sμ^3-CrFeCo cluster	IRIJAU	43
CpCr(CO)$_2$	2.243(2)	1.8	2	Sμ^3-CrFeCo cluster	IRIJAU	43
CpCr(CO)$_2$	2.333(1)	1.4	3a	η^2-DTDA-*exo*	LIXFUU	33
CpCr(CO)$_2$	2.3407(7)	1.3	3b	η^2-DTDA-*endo*	LIXFOO	33
CpCr(CO)$_2$	2.345(1)	1.3	3c	η^2-thione-*exo*	RATROU [d]	44
CpCr(CO)$_2$	2.345(1)	1.3	3a	η^2-DTDA-*exo*	SEKDES	34
CpCr(CO)$_2$	2.3463(9)	1.3	3a	η^2-DTDA-*exo*	SEKDES	34
CpCr(CO)$_2$	2.351(1)	1.3	3a	η^2-DTDA-*exo*	LIXFUU	33
CpCr(CO)$_2$	2.354(1)	1.3	3b	η^2-DTDA-*endo*	SEKDIW	34
CpCr(CO)$_2$	2.354(2)	1.3	3b	η^2-DTDA-*endo*	SEKDOC	34
CpCr(CO)$_2$	2.360(1)	1.3	3b	η^2-DTDA-*endo*	SEKDIW	34
CpCr(CO)$_2$	2.361(2)	1.3	3b	η^2-DTDA-*endo*	SEKDOC	34
CpCr(CO)$_2$	2.3688(7)	1.2	3b	η^2-DTDA-*endo*	LIXFOO	33
Cp*Cr(CO)$_2$	2.386(2)	1.2	4	η^2-S2-bridge	DACVIM	45
Cp*Cr(CO)$_2$	2.390(2)	1.2	4	η^2-S2-bridge	DACVIM	45
Cp*Cr(CO)$_2$	2.391(2)	1.2	4	η^2-S2-bridge	DACVIM	45
CpCr(CO)$_2$	2.396(2)	1.1	4	η^2-S2-bridge	FIPNUN	46
CpCr(CO)$_2$	2.396(2)	1.1	4	η^2-S2-bridge	FIPNUN	46
CpCr(CO)$_2$	2.4023(8)	1.1	5	S-C-S chelate	RATRUA	44
CpCr(CO)$_2$	2.4045(7)	1.1	6	Bridg. thiolate	FIVSAF	48
CpCr(CO)$_2$	2.406(2)	1.1	4	η^2-S2-bridge	FIPNUN	46
CpCr(CO)$_2$	2.4108(4)	1.1	5	S-C-S chelate	XUJHEP	49
Cp*Cr(CO)$_2$	2.413(2)	1.1	4	η^2-S2-bridge	DACVIM	45
CpCr(CO)$_2$	2.415(1)	1.1	4	η^2-S2-bridge	FIPNUN	46
CpCr(CO)$_2$	2.4158(9)	1.1	5	S-C-S chelate	RATRUA	44
CpCr(CO)$_2$	2.4158(9)	1.1	7	C=S, side-on	XUJHOZ	49
CpCr(CO)$_2$	2.4163(9)	1.1	6	Bridg. thiolate	FIVSAF	48
CpCr(CO)$_2$	2.4172(6)	1.1	5	S-C-S chelate	XUJHAL	49
CpCr(CO)$_2$	2.4188(9)	1.1	7	C=S, side-on	XUJHOZ	49
CpCr(CO)$_2$	2.4192(9)	1.1	6	Bridg. thiolate	FIVSAF	48
CpCr(CO)$_2$	2.4209(6)	1.1	5	S-C-S chelate	XUJGUE	49

CpCr(CO)$_2$	2.4209(5)	1.1	5	S-C-S chelate	XUJHEP	49
CpCr(CO)$_2$	2.4217(9)	1.1	5	S-C-S chelate	RATRUA	44
CpCr(CO)$_2$	2.4229(7)	1.1	6	Bridg. thiolate	FIVSAF	48
CpCr(CO)$_2$	2.4232(8)	1.1	5	S-C-S chelate	RATRUA	44
CpCr(CO)$_2$	2.4240(7)	1.0	5	S-C-S chelate	XUJHAL	49
CpCr(CO)$_2$	2.4265(6)	1.0	5	S-C-S chelate	XUJGUE	49
CpCr(CO)$_2$	2.431(2)	1.0	6	Bridg. thiolate	KUCWUA	50
CpCr(CO)$_3$	2.4406(6)	1.0	8	Term. thiolate	XUJGOY	49
Cp*Cr(CO)$_2$	2.442(2)	1.0	9	N-C-S chelate	INUWIX	51
CpCr(CO)$_2$	2.4421(7)	1.0	7	C=S, side-on	XUJHIT [d]	49
CpCr(CO)$_2$	2.447(1)	1.0	6	Bridg. thiolate	REGMOG	52
CpCr(CO)$_3$	2.448(3)	1.0	8	Term. thiolate	RATRIO	44
CpCr(CO)$_3$	2.4485(8)	1.0	8	Term. thiolate	MAKLOA	47
CpCr(CO)$_2$	2.449(2)	1.0	9	N-C-S chelate	HAKQAM	53
CpCr(CO)$_2$	2.4494(7)	1.0	7	C=S, side-on	XUJHIT	49
CpCr(CO)$_2$	2.450(3)	1.0	6	Bridg. thiolate	KUCWUA [f]	50
CpCr(CO)$_2$	2.4511(8)	1.0	10	Dative	CILYOM	54
CpCr(CO)$_2$	2.452(1)	1.0	6	Bridg. thiolate	REGMOG	52
CpCr(CO)$_2$	2.452(1)	1.0	6	Bridg. thiolate	REGMOG	52
Cp*Cr(CO)$_3$	2.452(2)	1.0	8	Term. thiolate	LAYWAK	55
CpCr(CO)$_2$	2.455(8)	1.0	11	S-P-S chelate	ICUMUO [e]	56
CpCr(CO)$_2$	2.455(1)	1.0	6	Bridg. thiolate	REGMOG	52
CpCr(CO)$_2$	2.457(2)	1.0	6	Bridg. thiolate	KUCWUA	50
CpCr(CO)$_2$	2.4584(8)	0.9	9	N-C-S chelate	HAKPUF [g]	53
CpCr(CO)$_3$	2.459(3)	0.9	8	Term. thiolate	RATRIO	44
Cp*Cr(CO)$_3$	2.4623(8)	0.9	8	Term. thiolate	INUWET	51
CpCr(CO)$_2$	2.466(3)	0.9	12	P=S, side-on	GABMUS [g]	57
CpCr(CO)$_3$	2.466(3)	0.9	8	Term. thiolate	CANYEV	40
CpCr(CO)$_2$	2.4663(8)	0.9	10	Dative	CILYOM [h]	54
CpCr(CO)$_2$	2.471(3)	0.9	6	Bridg. thiolate	KUCWUA	50
CpCr(CO)$_2$	2.472(2)	0.9	11	S-P-S chelate	GABNAZ [g]	57
CpCr(CO)$_2$	2.4757(7)	0.9	10	Dative	CILYOM [h]	54
CpCr(CO)$_2$	2.477(3)	0.9	11	S-P-S chelate	GABNAZ [g]	57
CpCr(CO)$_2$	2.481(9)	0.9	11	S-P-S chelate	ICUMUO [e,g]	56
CpCr(CO)$_2$	2.485(3)	0.9	12	P=S, side-on	PIDJAN [g]	58
CpCr(CO)$_2$	2.4866(8)	0.9	10	Dative	CILYOM [h]	54
Cp*Cr(CO)$_2$	2.488(1)	0.9	11	S-P-S chelate	GABNED [g]	57
Cp*Cr(CO)$_2$	2.490(1)	0.9	11	S-P-S chelate	GABNED [g]	57
Cp*Cr(CO)$_2$	2.490(2)	0.9	13	η^2-PS-bridge	GABPOP [g]	57
CpCr(CO)$_2$	2.492(2)	0.9	9	N-C-S chelate	MOSMAI [g]	59
CpCr(CO)$_2$	2.496(1)	0.8	12	P=S, side-on	GABPEF [g]	57
Cp*Cr(CO)$_2$	2.500(2)	0.8	13	η^2-PS-bridge	GABPOP [g]	57
CpCr(CO)$_2$	2.504(2)	0.8	12	P=S, side-on	WUMJET [g]	60
CpCr(CO)$_2$	2.507(2)	0.8	9	N-C-S chelate	MOSMAI [g]	59
Cp*Cr(CO)$_2$	2.508(1)	0.8	12	P=S, side-on	GABPAB [g]	57
CpCr(CO)$_2$	2.5111(9)	0.8	12	P=S, side-on	GABNUT [g]	57
CpCr(CO)$_2$	2.5156(7)	0.8	12	P=S, side-on	WUMJAP [g]	60
CpCr(CO)$_2$	2.517(2)	0.8	12	P=S, side-on	PIDJAN [g]	58

CpCr(CO)$_2$	2.521(1)	0.8	12	P=S side on	GABPIJ [g]	57
CpCr(CO)$_2$	2.547(1)	0.7	12	P=S side on	WOWKOI [g]	61
CpCr(CO)$_2$	2.551(1)	0.7	12	P=S side on	WOWKOI [g]	61

[a] Cp and Cp* usual meaning; Cp′ = η^5-C$_5$H$_4$C(O)CH$_3$. [b] Thirteen different structure classes are identified, with short descriptors; representative structure diagrams provided in the Supporting Information. [c] Cambridge Structural Database unique crystal structure identifier. [d] Disordered component excluded. [e] Disorder present in structure. [f] Bridging thiolates display a wide range of values. [g] Small ring strain present due to a stronger chromium-carbon or chromium-pnictide bond. [h] Dative bond found to be weaker than single covalent bond.

Table 2. Selected interatomic distances (Å) and angles (°) in **2** and **3** from crystallography and DFT calculations [a]

Parameter	**3**, X-ray [b]	**3**, DFT [c]	**2**$^-$, X-ray [d]	**2**$^-$, DFT [c]	**2**$_2$, X-ray [e]	**2**, DFT [c]	**2**$^+$, X-ray [f]	**2**$^+$, DFT [c]
S-N1	1.659(3)	1.651	1.697(6)	1.723	1.621	1.639	1.535	1.559
S-N3	1.675(3)	1.655	1.694(4)	1.724	1.628	1.639	*1.535*	1.559
N1-C7	1.325(4)	1.323	1.273(8)	1.302	1.329	1.327	1.369(6)	1.378
N2-C7	1.345(4)	1.347	1.379(7)	1.363	1.343	1.348	1.332	1.336
N2-C6	1.363(4)	1.341	1.393(8)	1.363	1.341	1.348	*1.332*	1.336
N3-C6	1.317(4)	1.328	1.286(7)	1.302	1.342	1.327	*1.369(6)*	1.378
C6-C8	1.486(5)	1.487	1.453(8)	1.498	1.485	1.482	1.450(6)	1.446
C7-C14	1.484(5)	1.485	1.470(8)	1.498	1.482	1.482	*1.450(6)*	1.446
S-Cr	2.4908(11)	2.552						
Cr-C(Cp$_{av}$) [g]	2.19(2)	2.20(2)						
Cr-C20	1.890(4)	1.850						
Cr-C21	1.860(4)	1.836						
Cr-C22	1.883(4)	1.851						
C20-O1	1.135(4)	1.147						
C21-O2	1.140(5)	1.150						
C22-O3	1.137(4	1.148						
N1-S-N3	106.13(15)	108.8	105.4(3)	105.8	110.5	109.7	112.3	113.2
S-N1-C7	115.2(2)	117.2	115.9(5)	113.8	117.1	117.7	119.3	118.1
N1-C7-N2	127.4(3)	128.5	122.6(5)	130.4	128.1	127.4	123.2	123.8
C7-N2-C6	117.2(3)	119.1	121.6(5)	116.3	119.1	120.1	122.4	123.1
N2-C6-N3	128.2(3)	128.5	121.4(5)	130.4	127.9	127.4	*123.2*	123.8
C6-N3-S	114.9(3)	117.0	116.2(4)	113.8	116.7	117.7	*119.3*	118.1
N1-S-Cr	109.25(11)	109.9						
N3-S-Cr	112.42(11)	108.8						
S-Cr-C20	80.69(11)	76.1						
S-Cr-C21	133.77(12)	135.9						
S-Cr-C22	75.73(11)	75.2						

[a] The atom numbering scheme adopted for all compounds is that employed for **3** as shown in Fig. 1. [b] This work; see also ref. 36. [c] This work, from geometry-optimized (U/R)B3PW91/6-31G(2d,p) DFT calculations verified by frequency calculations. [d] As the protonated imine, **2**H, ref. 68. [e] From ref. 67. [f] From the PF$_6^-$ salt, see ref. 68. Parameters in italics are identical duplicates due to two-fold rotation axis site symmetry in *C*2/*c*. [g] Errors for this parameter are standard deviations of the samples.

Table 3. Selected interatomic distances (Å) and angles (°) in **5a** and **6a** from crystallography and DFT calculations [a]

Parameter	**6a**, X-ray [b]	**6a**-*exo* DFT [c]	**6a**-*endo* DFT [c]	**5a⁻**, DFT [c]	**5a₂**, X-ray [d]	**5a**, DFT [c]	**5a⁺**, DFT [c]
S-N1	1.679(3)	1.694	1.690	1.728	1.628	1.640	1.563
S-N3	1.689(3)	1.695	1.699	1.737	1.643	1.652	1.570
N1-C8	1.361(4)	1.364	1.345	1.301	1.328	1.327	1.369
N3-C9	1.372(5)	1.289	1.296	1.293	1.321	1.310	1.362
N2-C8	1.311(5)	1.317	1.330	1.366	1.364	1.353	1.361
N2-C9	1.372(5)	1.362	1.355	1.352	1.329	1.336	1.303
C8-C10	1.473(5)	1.475	1.475	1.496	1.474	1.475	1.430
C9-C16	1.525(6)	1.530	1.530	1.526	1.530	1.532	1.540
Cr-S	2.2965(11)	2.303	2.348				
Cr-N1	2.098(3)	2.091	2.072				
Cr-C(Cp$_{av}$) [e]	2.18(4)	2.19(4)	2.19(4)				
Cr-C6	1.837(5)	1.827	1.830				
Cr-C7	1.848(4)	1.833	1.835				
C6-O1	1.144(5)	1.152	1.152				
C7-O2	1.139(4)	1.151	1.151				
N1-S-N3	107.95(16)	107.8	105.7	105.6	109.3	109.4	112.5
S-N1-C8	116.7(3)	115.7	116.5	113.8	119.1	118.6	119.6
N1-C8-N2	128.0(3)	127.2	125.8	129.9	126.8	126.7	122.4
C8-N2-C9	117.6(3)	118.6	117.4	115.0	117.3	118.8	121.5
N2-C9-N3	132.3(4)	131.9	132.3	133.2	131.9	130.9	127.9
C9-N3-S	114.9(3)	114.0	112.4	111.6	115.4	115.8	116.2
N1-S-Cr	61.41(11)	60.8	59.1				
S-N1-Cr	73.94(12)	74.1	76.5				
S-Cr-N1	44.65(9)	45.0	44.4				
S-Cr-C6	88.65(12)	87.7	86.7				
S-Cr-C7	116.91(12)	115.1	114.7				
N1-Cr-C7	89.19(15)	88.2	86.3				
N1-Cr-C6	119.26(15)	119.6	115.7				

[a] The atom numbering scheme for all compounds is that employed for **6a** as shown in Fig. 2. [b] This work; see also refs. 33, 34. [c] This work, from geometry-optimized (U/R)B3PW91/6-31G(2d,p) DFT calculations verified by frequency calculations. [d] Taken from ref. 62; values are averages for the two independent radicals in the dimer structure. [e] Errors for this parameter are standard deviations of the samples.

Table 4. Selected interatomic distances (Å) and angles (°) in **5b** and **6b** from crystallography and DFT calculations [a]

Parameter	**6b**, X-ray [b]	**6b**-*exo* DFT [c]	**6b**-*endo* DFT [c]	**5b**$^-$, DFT [c]	**5b**$_2$, X-ray [d]	**5b**, DFT [c]	**5b**$^+$, DFT [c]
S-N1	1.689(4)	1.692	1.688	1.728	1.625	1.639	1.560
S-N3	1.694(4)	1.693	1.697	1.737	1.645	1.651	1.569
N1-C8	1.360(6)	1.368	1.349	1.301	1.334	1.331	1.373
N3-C9	1.276(6)	1.291	1.297	1.293	1.318	1.311	1.368
N2-C8	1.324(6)	1.320	1.332	1.367	1.361	1.355	1.371
N2-C9	1.369(6)	1.359	1.353	1.352	1.328	1.335	1.297
C8-C10	1.468(6)	1.466	1.466	1.493	1.463	1.466	1.414
C9-C17	1.520(7)	1.530	1.530	1.525	1.529	1.531	1.537
Cr-S	2.2987(14)	2.302	2.345				
Cr-N1	2.098(3)	2.090	2.076				
Cr-C(Cp$_{av}$) [e]	2.19(4)	2.20(5)	2.19(4)				
Cr-C6	1.829(5)	1.825	1.830				
Cr-C7	1.845(5)	1.832	1.833				
C6-O1	1.161(5)	1.152	1.152				
C7-O2	1.137(6)	1.151	1.152				
N1-S-N3	107.30(19)	108.06	106.07	105.59	109.20	109.58	112.91
S-N1-C8	117.4(3)	115.68	116.56	113.80	119.24	118.53	119.55
N1-C8-N2	126.6(4)	126.90	125.61	129.88	126.27	126.46	122.16
C8-N2-C9	117.8(4)	118.85	117.68	115.00	117.48	118.82	121.41
N2-C9-N3	132.7(4)	131.98	132.33	133.24	131.06	130.98	128.22
C9-N3-S	114.4(3)	113.92	112.42	111.59	115.35	115.63	115.75
N1-S-Cr	61.31(13)	60.86	59.35				
S-N1-Cr	73.80(14)	74.14	76.28				
S-Cr-N1	44.89(11)	45.00	44.37				
S-Cr-C6	86.38(15)	87.69	86.63				
S-Cr-C7	114.82(15)	115.23	113.84				
N1-Cr-C7	89.38(18)	88.11	86.16				
N1-Cr-C6	118.73(18)	119.35	116.15				

[a] The atom numbering scheme for all compounds is that employed for **6a** as shown in Fig. 2. [b] This work. [c] This work, from geometry-optimized (U/R)B3PW91/6-31G(2d,p) DFT calculations verified by frequency calculations. [d] Taken from ref. 62; values are averages for the two independent radicals in the dimer structure. [e] Errors for this parameter are standard deviations of the samples.

Table 5. Crystal data and structure refinement parameters for **3**, **6a** and **6b**

Parameter, unit(s)	3	6a	6b
Formula	$C_{22}H_{15}CrN_3O_3S$	$C_{16}H_{10}CrF_3N_3O_2S$	$C_{17}H_{12}CrF_3N_3O_3S$
Formula weight, amu	453.43	417.33	447.36
Temperature, K	223(2)	223(2)	223(2)
Radiation / λ, Å		Mo Kα / 0.71073	
Crystal system	Monoclinic	Triclinic	Monoclinic
Space group	$P2_1/n$	$P\bar{1}$	$P2_1/c$
Unit cell dimensions: a, Å	8.4611(17)	8.0929(8)	8.1311(7)
b, Å	20.509(4)	10.3160(10)	24.284(2)
c, Å	11.757(2)	11.2405(11)	9.1025(8)
α, °	90.000	70.032(2)	90.000
β, °	104.453(7)	72.076(2)	97.218(2)
γ, °	90.000	82.375(2)	90.000
Volume, Å^3	1975.6(7)	838.81(14)	1783.1(3)
Z	4	2	4
D_c, g/cm^3	1.524	1.652	1.666
μ, mm^{-1}	0.715	0.854	0.813
Absorption correction		Semi-empirical from equivalents	
Max. and min. transmission	0.9584, 0.7931	0.9348, 0.7838	0.9682, 0.6865
F(000)	928	420	904
Crystal size, mm^3	0.34 x 0.24 x 0.34	0.30 x 0.20 x 0.34	0.50 x 0.08 x 0.04
Theta range for data collection, °	1.99 to 27.50	2.01 to 27.50	1.68 to 24.99
Index ranges	$-10 \leq h \leq 7$, $-25 \leq k \leq 26$, $-15 \leq l \leq 15$	$-10 \leq h \leq 10$, $-13 \leq k \leq 13$, $-14 \leq l \leq 14$	$-9 \leq h \leq 9$, $-28 \leq k \leq 20$, $-10 \leq l \leq 10$
Total / Independent rfls.	13844 / 4526	11159 / 3845	10124 / 3143
R_{int} =	0.0483	0.0387	0.0697
Completeness to θ = 25.25°, %	99.9	99.6	99.9
Data / restraints / parameters	4526 / 0 / 271	3845 / 0 / 235	3143 / 0 / 254
Goodness-of-fit on F^2	1.158	1.146	1.094
Final R indices [I>2σ(I)]	R_1 = 0.0677, wR_2 = 0.0882	R_1 = 0.0663, wR_2 = 0.0865	R_1 = 0.0634, wR_2 = 0.1257
R indices (all data)	R_1 = 0.1439, wR_2 = 0.1525	R_1 = 0.1454, wR_2 = 0.1560	R_1 = 0.0962, wR_2 = 0.1366
Largest diff. peak and hole, e Å^{-3}	0.739, -0.304	0.420, -0.259	0.488, -0.336

Coordination complexes of thiazyl rings. Synthesis, structure and DFT computational analysis of CpCr(CO)$_x$ (x = 2,3) complexes of fluorinated and non-fluorinated $1\lambda^3$-1,2,4,6-thiatriazinyls, with differing Cr—S bond orders.

Chwee Ying Ang, Seah Ling Kuan, Geok Kheng Tan, Lai Yoong Goh, Tracey L. Roemmele, Xin Yu and René T. Boeré

Graphical Abstract

Coordination complexes of thiazyl rings. Synthesis, structure and DFT computational analysis of CpCr(CO)$_x$ (*x* = 2,3) complexes of fluorinated and non-fluorinated 1λ^3-1,2,4,6-thiatriazinyls, with differing Cr—S bond orders.

Chwee Ying Ang, Seah Ling Kuan, Geok Kheng Tan, Lai Yoong Goh, Tracey L. Roemmele, Xin Yu and René T. Boeré

Supporting Information

Figure S1. Bond-order structure diagrams – representative examples.

Class, Descriptor, Example structure with CSD "refcode"
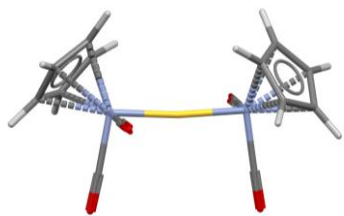
Class 1, Linear bridging monosulfide (S_1), SCPDCC
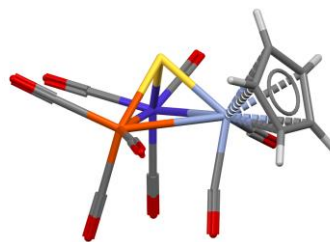
Class 2, $S\mu^3$-CrFeCo cluster, IRIJAU
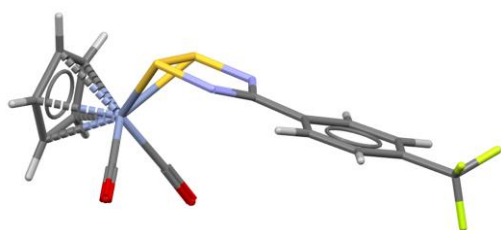
Class 3a, η^2-DTDA-*exo,* LIXFUU
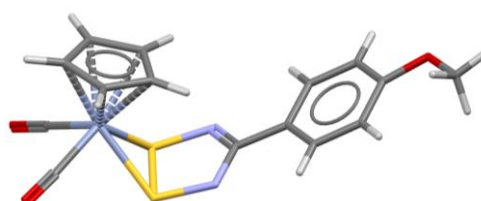
Class 3b, η^2-DTDA-*endo,* LIXFOO
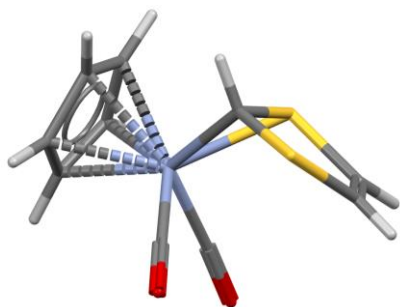
Class 3c, η^2-thione-*exo,* RATROU
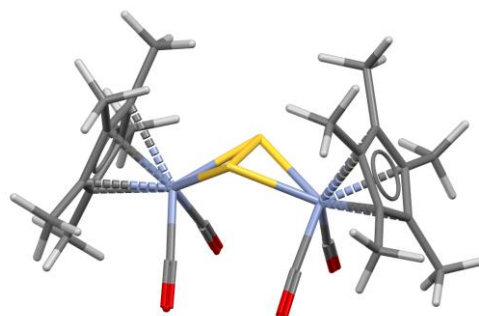
Class 4, η^2-S2-bridge, DACVIM
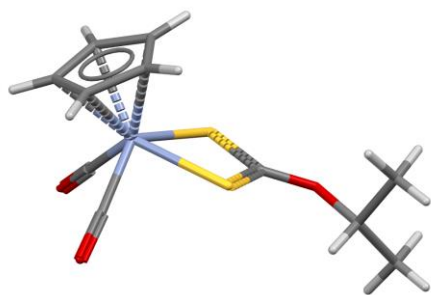
Class 5, S-C-S chelate, RATRUA
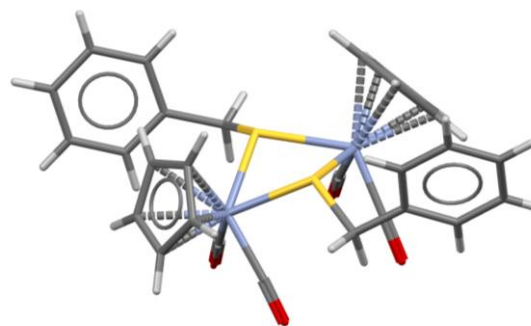
Class 6, Bridging thiolate, FIVSAF
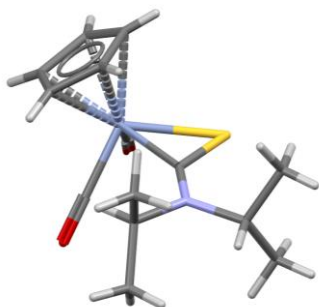
Class 7, C=S, side-on, Xᴜᴊʜᴏᴢ
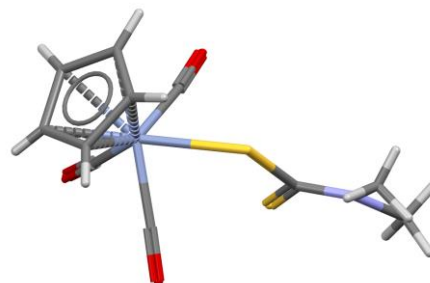
Class 8, Terminal thiolate, Xᴜᴊɢᴏʏ
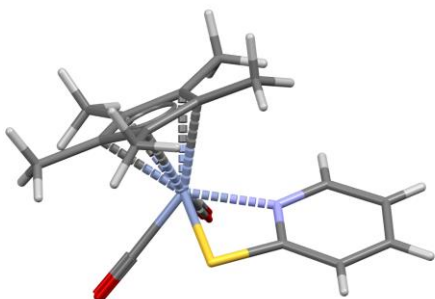
Class 9, N-C-S chelate, Iɴᴜᴡɪx
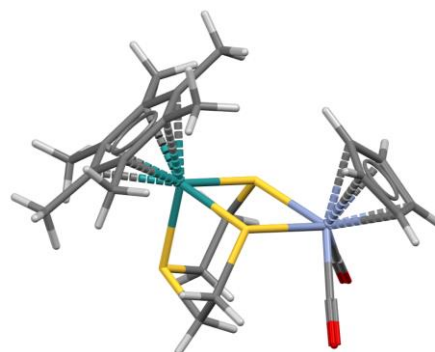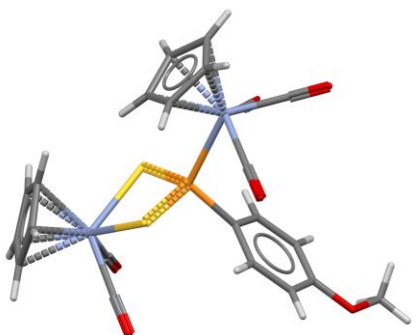
Class 10, Dative, Cɪʟʏᴏᴍ

Class 11, S-P-S chelate, Gᴀʙɴᴀᴢ

Class 12, P=S, side-on, Gᴀʙᴍᴜs

Class 13, η^2-PS-bridge, Gᴀʙᴘᴏᴘ

Figure S2. Graph of the Cr–S bond distances taken from Table 1 and binned to 0.01 Å groups.

Figure S3. Histogram of CpCr(CO)$_x$-N distances.
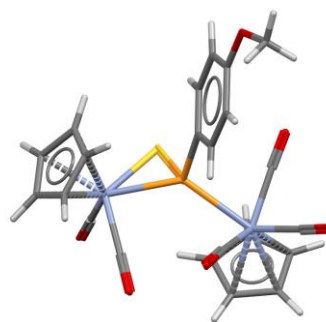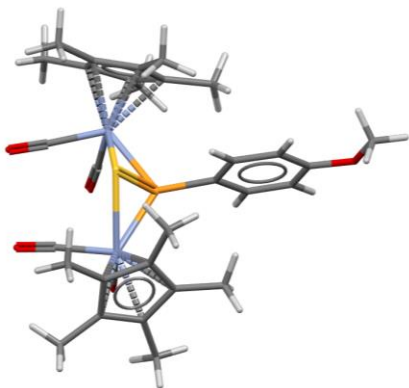
Figure S4. Histogram of CSD structures containing Cr—N bonds showing the bond distances.
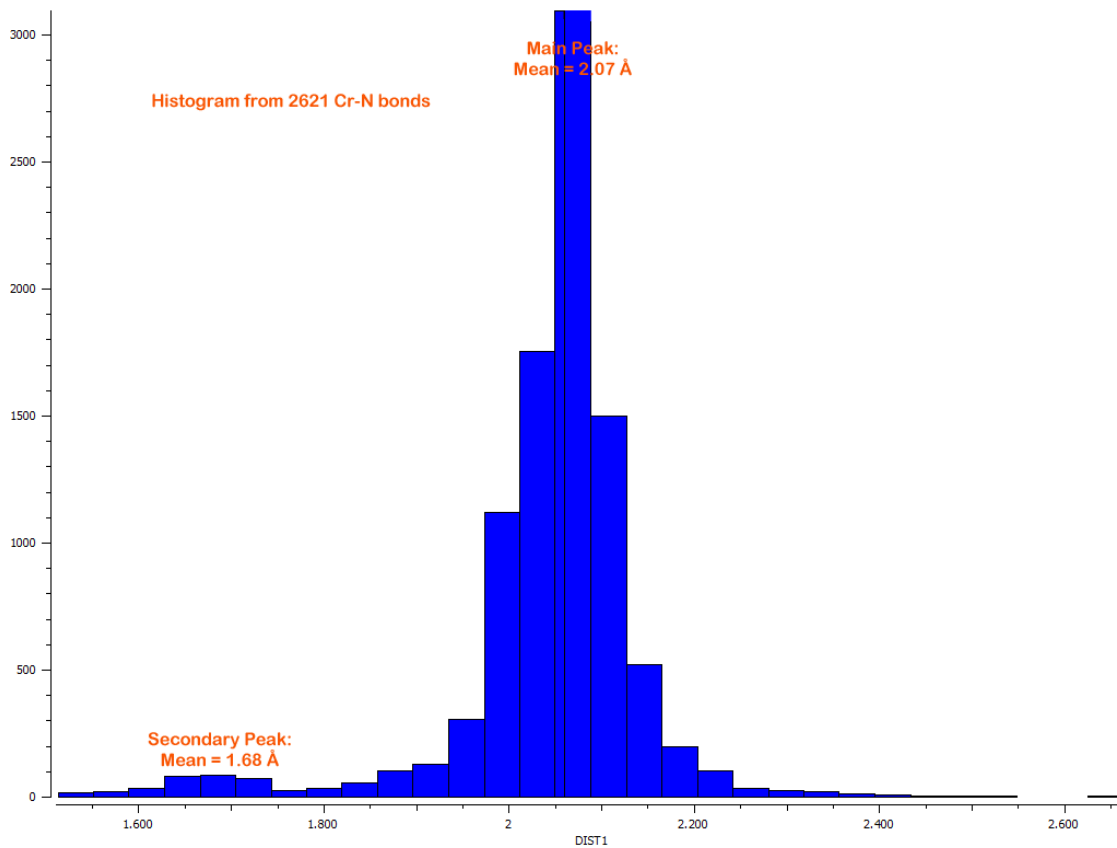
Figure S5 Histogram of CSD chromium nitride structures showing the Cr≡N bond distances (subset, coloured red, of the "secondary peak" in Figure S4.)
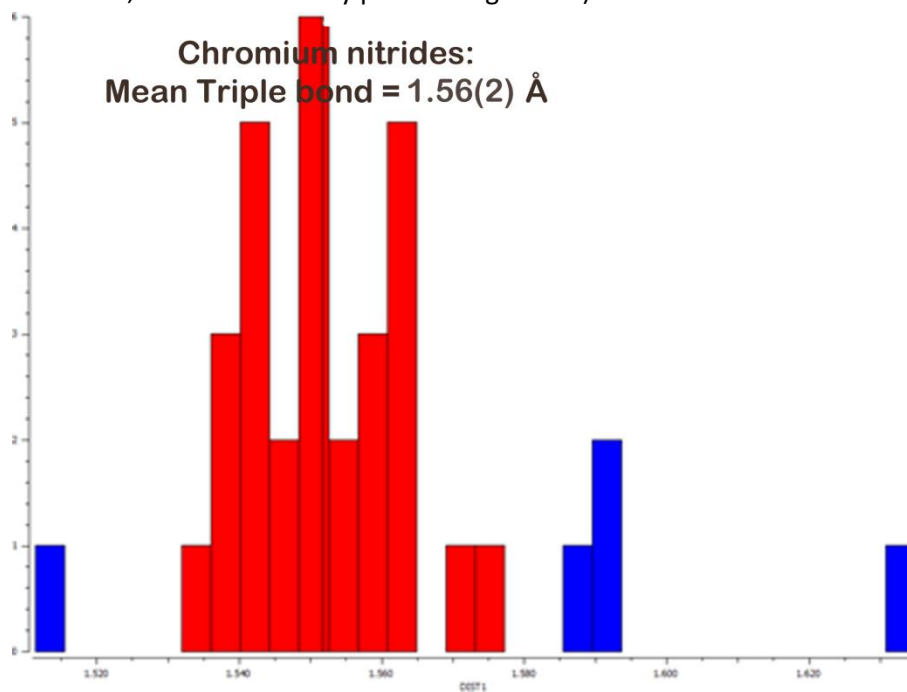
Figure S6 Histogram of CSD chromium imido complexes showing the Cr=N bond distances (subset of the "secondary peak" in Figure S4.

Cr=NR Imido Complexes
Mean short Cr-N distances: 1.64(2) Å
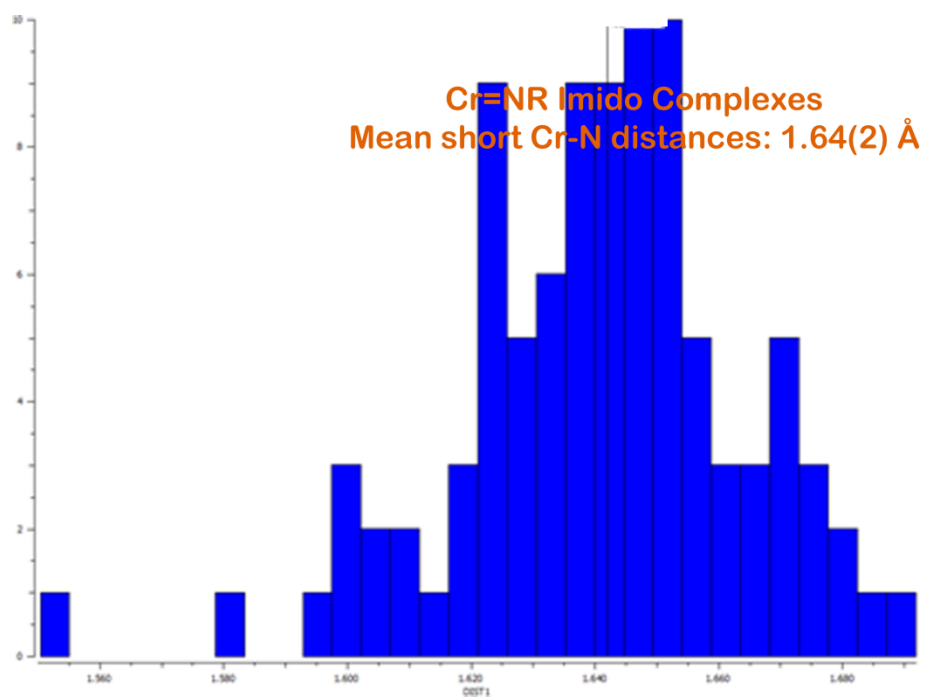
Table S1. RB3PW91/ 6-31G(2d,p) Geometry and Cartesian Coordinates for **3.**

Label	Symbol	NA	NB	NC	Bond	Angle	Dihedral	X	Y	Z
1	Cr							-2.5603530	-0.0850930	0.1895670
2	S	1			2.5517317			-0.5354420	-0.0193810	-1.3618040
3	N	2	1		1.6512782	109.9281634		0.4283510	-1.3313570	-1.0851420
4	N	3	2	1	2.4043209	91.2337379	-111.0327272	2.1467090	0.0638030	-0.1462420
5	N	2	1	3	1.6547700	108.8098038	-119.0947643	0.3311980	1.3553800	-1.0499850
6	O	1	2	3	2.9949259	77.6687715	65.2587858	-0.2917290	0.2638510	2.1134080
7	O	1	2	3	2.9855137	136.4275319	4.9114463	-3.5040550	-1.8012620	2.4428940
8	O	1	2	3	2.9964849	76.6747590	-54.0094590	-2.6428480	-2.7555530	-1.1671790
9	C	1	2	3	2.2301402	76.2180611	-179.2548896	-2.8746000	1.7645280	-1.0161180
10	H	9	1	2	1.0811500	123.7239937	-10.5762818	-2.1230670	2.1934340	-1.6642870
11	C	9	1	2	1.4172677	70.8825233	-130.5896177	-3.0378180	2.0726060	0.3575980
12	H	11	9	1	1.0805487	125.7924549	119.2041125	-2.4453610	2.7785930	0.9216570
13	C	11	9	1	1.4175967	107.8567725	-61.0372454	-4.1156190	1.2958870	0.8522020
14	H	13	11	9	1.0810027	125.9143134	-179.0160057	-4.4988070	1.3138970	1.8628500
15	C	13	11	9	1.4267876	108.1295249	0.6214387	-4.6118450	0.4928840	-0.2176900
16	H	15	13	11	1.0807247	126.0635429	-179.2065968	-5.4402120	-0.1990260	-0.1626040
17	C	9	1	15	1.4193945	69.8781152	-38.0744268	-3.8336340	0.7806350	-1.3723330
18	H	17	9	1	1.0808566	125.9436875	-119.4213672	-3.9600640	0.3435480	-2.3527520
19	C	5	2	1	1.3279113	116.9791195	109.9859342	1.5127450	1.2026450	-0.4634980
20	C	3	2	1	1.3227059	117.2050273	-109.3210192	1.5927720	-1.1130180	-0.4969220
21	C	6	1	15	1.1473234	2.7876804	-168.0485421	-1.1251360	0.1062080	1.3407940
22	C	7	1	21	1.1498035	0.8845849	-51.7012972	-3.1252610	-1.1492350	1.5748940
23	C	8	1	22	1.1481797	3.0249673	-106.6300072	-2.5507300	-1.7358370	-0.6475540
24	C	19	5	2	1.4867704	115.3866462	-177.8348191	2.2386040	2.4628380	-0.1544210
25	C	24	19	5	1.3980874	120.0589242	174.1741606	3.4330600	2.4231040	0.5710750
26	C	24	19	5	1.3990398	120.7755963	-5.7805184	1.7406990	3.6987800	-0.5808600
27	C	25	24	19	1.3893094	120.3478157	-179.7118617	4.1131580	3.5975200	0.8683870
28	H	25	24	19	1.0832325	118.4282640	-0.1303085	3.8061750	1.4600710	0.8977940
29	C	26	24	19	1.3883182	120.4019859	-179.8928873	2.4260100	4.8705650	-0.2898340
30	H	26	24	19	1.0840600	118.8377319	-0.4662626	0.8177350	3.7228200	-1.1489670
31	C	27	25	24	1.3922951	120.1663049	-0.4386845	3.6137100	4.8235560	0.4372570
32	H	27	25	24	1.0858603	119.7473193	179.6505356	5.0370730	3.5558080	1.4373630
33	H	29	26	24	1.0859267	119.8179992	179.5757746	2.0345100	5.8241250	-0.6314300
34	H	31	27	25	1.0860751	120.1170879	-179.7329002	4.1482930	5.7407650	0.6664030
35	C	20	3	2	1.4853597	115.3164598	177.9909450	2.4051540	-2.3267290	-0.2263030
36	C	35	20	3	1.3994609	120.4999135	-6.9765890	1.8739320	-3.6017320	-0.4513840
37	C	35	20	3	1.3980180	120.2063754	173.0365775	3.7112510	-2.2054740	0.2572900
38	C	36	35	20	1.3881015	120.2889358	-179.9035006	2.6363160	-4.7330630	-0.1950900
39	H	36	35	20	1.0841727	118.8515073	0.0673122	0.8606420	-3.6874100	-0.8273270
40	C	37	35	20	1.3892951	120.2925661	179.9909109	4.4726200	-3.3394880	0.5112000
41	H	37	35	20	1.0832200	118.4899415	-0.2873427	4.1109240	-1.2123410	0.4225590
42	C	40	37	35	1.3923110	120.1297604	-0.0852437	3.9376070	-4.6051570	0.2867610
43	H	38	36	35	1.0858078	119.7858708	179.8373864	2.2150680	-5.7183980	-0.3701430
44	H	40	37	35	1.0858845	119.7815850	179.8828785	5.4868690	-3.2356230	0.8849060
45	H	42	40	37	1.0861337	120.0754146	-179.8991072	4.5330500	-5.4911540	0.4871190

Table S2. RB3PW91/ 6-31G(2d,p) Geometry and Cartesian Coordinates for **2**⁻.

Label	Symbol	NA	NB	NC	Bond	Angle	Dihedral	X	Y	Z
1	S							0.0000620	2.9739430	-0.1715580
2	N	1			1.7234338			1.3747840	1.9696300	0.0962460
3	N	2	1		2.4189602	88.5315487		-0.0000480	0.0520160	-0.4366350
4	N	1	2	3	1.7237267	105.8206199	24.6638735	-1.3749900	1.9696060	0.0963470
5	C	4	1	2	1.3020947	113.7792920	-27.6960767	-1.1576170	0.7077830	-0.1403010
6	C	2	1	4	1.3020864	113.7914514	27.6963464	1.1575310	0.7077810	-0.1403280
7	C	5	4	1	1.4982500	114.6281517	-175.1188993	-2.3686340	-0.1667800	-0.0248430
8	C	7	5	4	1.3975089	120.6073005	-178.1666564	-2.2698720	-1.5476880	-0.2155530
9	C	7	5	4	1.3998790	120.9122258	2.5782468	-3.6255870	0.3793980	0.2604990
10	C	8	7	5	1.3922704	120.7768137	-179.3512024	-3.3952910	-2.3620340	-0.1223350
11	H	8	7	5	1.0838858	117.3582995	0.6526137	-1.2884460	-1.9510440	-0.4367210
12	C	9	7	5	1.3889729	120.8052132	179.6399828	-4.7481080	-0.4326060	0.3597050
13	H	9	7	5	1.0849360	117.6755813	-0.4591093	-3.6881120	1.4532860	0.4017130
14	C	10	8	7	1.3917454	120.3277185	-0.2415243	-4.6396200	-1.8105910	0.1683730
15	H	10	8	7	1.0877869	119.7125345	179.9428734	-3.2987310	-3.4347330	-0.2748910
16	H	12	9	7	1.0876958	119.7512464	179.7521734	-5.7157680	0.0094850	0.5861380
17	H	14	10	8	1.0874291	120.3797596	-179.8205215	-5.5186730	-2.4462090	0.2442520
18	C	6	2	1	1.4982154	114.6317242	175.1123871	2.3685840	-0.1666910	-0.0250080
19	C	18	6	2	1.3998855	120.9133645	-2.4568497	3.6251170	0.3792560	0.2626480
20	C	18	6	2	1.3975086	120.6067666	178.2899898	2.2703320	-1.5472900	-0.2182000
21	C	19	18	6	1.3889693	120.8055426	-179.6392331	4.7476950	-0.4326810	0.3617070
22	H	19	18	6	1.0849354	117.6753599	0.4584591	3.6872680	1.4529170	0.4057360
23	C	20	18	6	1.3922749	120.7770127	179.3473714	3.3958340	-2.3615530	-0.1251920
24	H	20	18	6	1.0838849	117.3605690	-0.6513543	1.2892630	-1.9505100	-0.4411880
25	C	23	20	18	1.3917443	120.3280822	0.2459114	4.6397200	-1.8103610	0.1678730
26	H	21	19	18	1.0876947	119.7506533	-179.7476783	5.7149940	0.0092250	0.5900300
27	H	23	20	18	1.0877866	119.7117981	-179.9391404	3.2996680	-3.4339990	-0.2797600
28	H	25	23	20	1.0874280	120.3802709	179.8169589	5.5188220	-2.4459220	0.2436460

Table S3. UB3PW91/ 6-31G(2d,p) Geometry and Cartesian Coordinates for **2˙**.

Label	Symbol	NA	NB	NC	Bond	Angle	Dihedral	X	Y	Z
1	S							0.0000000	2.8927140	-0.0001220
2	N	1			1.6387374			1.3400050	1.9493970	-0.0001530
3	N	2	1		2.3982890	91.1758561		-0.0000030	-0.0396150	-0.0000120
4	N	1	2	3	1.6387294	109.7115424	0.0020140	-1.3399980	1.9494010	0.0000340
5	C	4	1	2	1.3266331	117.7008406	-0.0050323	-1.1681370	0.6339470	0.0000060
6	C	2	1	4	1.3266233	117.7007154	0.0000000	1.1681430	0.6339530	-0.0000560
7	C	5	4	1	1.4817326	115.9917954	-179.9943536	-2.4046570	-0.1824780	0.0000190
8	C	7	5	4	1.3985793	120.3430524	179.9864382	-2.3292150	-1.5790210	-0.0002940
9	C	7	5	4	1.3999908	120.3704181	-0.0126776	-3.6608710	0.4355030	0.0003260
10	C	8	7	5	1.3889875	120.2829139	-179.9987307	-3.4891410	-2.3431270	-0.0003080
11	H	8	7	5	1.0831075	118.7100782	0.0006964	-1.3525800	-2.0473220	-0.0005330
12	C	9	7	5	1.3876959	120.2766792	179.9994928	-4.8176640	-0.3310020	0.0003270
13	H	9	7	5	1.0841019	118.9337945	-0.0005866	-3.7126840	1.5183660	0.0005630
14	C	10	8	7	1.3923409	120.1354903	-0.0007643	-4.7353090	-1.7220970	0.0000060
15	H	10	8	7	1.0857102	119.7576236	179.9992192	-3.4206390	-3.4266740	-0.0005650
16	H	12	9	7	1.0856515	119.7635513	179.9992277	-5.7874900	0.1569290	0.0005790
17	H	14	10	8	1.0859746	120.0735140	-179.9994965	-5.6415460	-2.3204910	0.0000030
18	C	6	2	1	1.4817309	115.9920182	-179.9962098	2.4046570	-0.1824780	0.0000000
19	C	18	6	2	1.3999921	120.3701703	0.0039014	3.6608730	0.4355020	0.0000330
20	C	18	6	2	1.3985784	120.3432499	-179.9965515	2.3292120	-1.5790200	0.0000300
21	C	19	18	6	1.3876951	120.2765812	179.9994949	4.8176630	-0.3310060	0.0000960
22	H	19	18	6	1.0841019	118.9337727	-0.0004775	3.7126870	1.5183650	0.0000090
23	C	20	18	6	1.3889878	120.2828812	-179.9996413	3.4891370	-2.3431280	0.0000900
24	H	20	18	6	1.0831070	118.7101537	0.0000000	1.3525770	-2.0473200	0.0000100
25	C	23	20	18	1.3923404	120.1355286	0.0000000	4.7353060	-1.7221010	0.0001250
26	H	21	19	18	1.0856519	119.7634514	-179.9997089	5.7874900	0.1569240	0.0001260
27	H	23	20	18	1.0857103	119.7576106	-180.0000000	3.4206330	-3.4266750	0.0001110
28	H	25	23	20	1.0859743	120.0735707	180.0000000	5.6415420	-2.3204960	0.0001760

Table S4. RB3PW91/ 6-31G(2d,p) Geometry and Cartesian Coordinates for **2**[+].

Label	Symbol	NA	NB	NC	Bond	Angle	Dihedral	X	Y	Z
1	S							-0.0000040	2.7997370	0.0000350
2	N	1			1.5593814			-1.3020930	1.9416960	-0.0002480
3	N	2	1		2.3937954	90.4311617		0.0000010	-0.0669870	-0.0001630
4	N	1	2	3	1.5593957	113.2322890	-0.0033798	1.3020950	1.9416850	0.0002840
5	C	3	2	1	1.3356579	94.4993220	-0.0016237	1.1743190	0.5693770	0.0000450
6	C	3	2	1	1.3356291	28.5948157	179.9839717	-1.1743000	0.5693480	-0.0001420
7	C	5	3	2	1.4458293	119.8823346	-179.9919803	2.4049190	-0.1896000	0.0000110
8	C	7	5	3	1.4082312	119.9970830	0.0014054	2.3639460	-1.5972350	-0.0002710
9	C	7	5	3	1.4091585	120.1805629	-179.9991810	3.6473370	0.4753250	0.0002470
10	C	8	7	5	1.3825250	119.8473391	179.9994613	3.5425580	-2.3199030	-0.0003140
11	H	8	7	5	1.0829072	119.3625102	0.0000000	1.4051050	-2.1005360	-0.0004600
12	C	9	7	5	1.3838568	119.8367881	-179.9995830	4.8208100	-0.2581740	0.0002040
13	H	9	7	5	1.0835896	119.8201624	0.0007690	3.6788230	1.5584570	0.0004670
14	C	12	9	7	1.3953157	119.9266475	0.0000000	4.7701310	-1.6525690	-0.0000750
15	H	10	8	7	1.0845298	119.9843697	180.0000000	3.5135960	-3.4040460	-0.0005270
16	H	12	9	7	1.0844286	119.9258046	179.9996103	5.7777160	0.2520380	0.0003790
17	H	14	12	9	1.0855371	119.7100012	-179.9997049	5.6928060	-2.2244620	-0.0001030
18	C	6	3	2	1.4458302	119.8843122	179.9975096	-2.4049170	-0.1896030	-0.0000560
19	C	18	6	3	1.4091556	120.1814990	-179.9898595	-3.6473290	0.4753270	-0.0002490
20	C	18	6	3	1.4082320	119.9962200	0.0113478	-2.3639530	-1.5972390	0.0002470
21	C	19	18	6	1.3838589	119.8367437	-179.9991848	-4.8208070	-0.2581680	-0.0001480
22	H	19	18	6	1.0835886	119.8204581	0.0017447	-3.6788150	1.5584580	-0.0004910
23	C	20	18	6	1.3825254	119.8475005	179.9983977	-3.5425680	-2.3199030	0.0003620
24	H	20	18	6	1.0829073	119.3624976	-0.0009503	-1.4051150	-2.1005460	0.0003980
25	C	21	19	18	1.3953143	119.9268066	0.0007885	-4.7701380	-1.6525620	0.0001610
26	H	21	19	18	1.0844275	119.9256037	-179.9991009	-5.7777080	0.2520510	-0.0003110
27	H	23	20	18	1.0845297	119.9844280	-179.9991631	-3.5136110	-3.4040460	0.0006090
28	H	25	21	19	1.0855365	119.7100580	179.9996566	-5.6928160	-2.2244490	0.0002450

Table S5. RB3PW91/ 6-31G(2d,p) Geometry and Cartesian Coordinates for **6a**-*exo*.

Label	Symbol	NA	NB	NC	Bond	Angle	Dihedral	X	Y	Z
1	Cr							1.7947970	-0.4746930	0.1218290
2	S	1			2.3026258			0.3861250	-1.2127950	-1.5433840
3	N	2	1		1.6937121	60.8422201		0.2669150	0.3911040	-1.0123870
4	N	3	2	1	2.4013719	89.9899370	-123.1606158	-2.0499450	0.0438500	-0.4849770
5	N	2	1	3	1.6952934	111.9969617	-98.7387552	-0.9411590	-2.0643710	-0.9211660
6	F	5	2	1	2.5954161	177.0649052	165.4069184	-3.0320520	-3.3561940	-0.0871730
7	F	4	3	2	2.8231225	131.2867123	60.9260473	-3.3047710	-1.7338160	1.3137270
8	F	4	3	2	2.7674064	146.9264843	-7.9373716	-4.2346370	-1.6480290	-0.6373070
9	O	1	3	2	2.9779824	120.4309167	-50.8462063	1.3465010	-3.0579730	1.5339460
10	O	1	3	2	2.9826006	89.2065625	-129.5868497	0.4826420	0.5508980	2.5961610
11	C	1	3	2	2.2634638	87.0366870	113.9217356	3.2153010	0.9424520	-0.9256140
12	H	11	1	3	1.0803305	123.2379905	11.1767003	2.8834340	1.7711050	-1.5341470
13	C	11	1	3	1.4154987	68.8836655	130.9223096	3.4084560	0.9705760	0.4763620
14	H	13	11	1	1.0808215	125.9862130	-120.6232318	3.3105990	1.8380230	1.1136490
15	C	13	11	1	1.4257018	107.8900870	61.0884698	3.7935760	-0.3377710	0.8917370
16	H	15	13	11	1.0806159	126.1033471	177.5597899	4.0503260	-0.6365940	1.8979750
17	C	15	13	11	1.4249666	107.6817236	-1.2562673	3.8056050	-1.1724910	-0.2630910
18	H	17	15	13	1.0808525	126.1002723	178.5749849	4.0770010	-2.2183670	-0.2901040
19	C	11	1	3	1.4114915	70.6962529	-109.3431790	3.4460280	-0.3725870	-1.3835940
20	H	19	11	1	1.0816002	125.9801694	120.7177377	3.3670970	-0.7118780	-2.4075620
21	C	9	1	3	1.1515401	1.2896584	2.8788373	1.4959910	-2.0607150	0.9779120
22	C	10	1	21	1.1509886	1.7334426	-98.0627020	0.9584390	0.1574130	1.6247900
23	C	4	3	2	1.3171476	26.8946257	-173.8787765	-0.9744920	0.7929390	-0.6159130
24	C	5	2	1	1.2891792	113.9886863	83.2088343	-1.9102830	-1.3103430	-0.5284530
25	C	23	4	3	1.4752579	117.2029453	179.7886669	-1.1113490	2.2291290	-0.3076690
26	C	25	23	4	1.3991646	120.9782974	-161.4646370	-0.1722180	3.1575870	-0.7699030
27	H	26	25	23	1.0836857	118.9815242	1.3328167	0.6528180	2.8102640	-1.3806870
28	C	26	25	23	1.3883581	120.1946299	179.6211455	-0.3211710	4.5064480	-0.4767730
29	H	28	26	25	1.0855819	119.9292329	-179.3208787	0.4040570	5.2244580	-0.8469000
30	C	28	26	25	1.3930865	119.9584389	0.1648450	-1.4065860	4.9375970	0.2826180
31	C	30	28	26	1.3936273	120.1067799	-0.3402865	-2.3472160	4.0179570	0.7426990
32	H	31	30	28	1.0854121	120.0860228	-179.9812745	-3.1929430	4.3542930	1.3340900
33	C	31	30	28	1.3875028	120.1127356	0.1159076	-2.2044950	2.6696460	0.4479920
34	H	33	31	30	1.0838285	121.4454504	-179.9933595	-2.9230200	1.9359760	0.7945960
35	C	24	5	2	1.5297782	115.7976784	179.0778605	-3.1391220	-2.0374480	0.0206320
36	H	30	28	26	1.0859339	119.9272079	179.9275985	-1.5219600	5.9926110	0.5125890

Table S6. RB3PW91/ 6-31G(2d,p) Geometry and Cartesian Coordinates for **6a**-*endo*.

Label	Symbol	NA	NB	NC	Bond	Angle	Dihedral	X	Y	Z
1	C							-0.6276480	-0.5006270	1.9478580
2	H	1			1.0812066			0.3924410	-0.1471770	2.0070120
3	C	1	2		1.4217904	125.8799277		-1.7954880	0.2925560	2.1166730
4	H	3	1	2	1.0805698	126.0191535	-3.2361025	-1.8192990	1.3416740	2.3743850
5	C	3	1	2	1.4280808	107.7233355	179.1474001	-2.9284490	-0.5586320	1.9397740
6	H	5	3	1	1.0808531	126.1610883	177.9621579	-3.9652630	-0.2682670	2.0343700
7	C	5	3	1	1.4222969	107.6479804	-1.1517167	-2.4456480	-1.8618000	1.6371440
8	H	7	5	3	1.0808423	126.0902007	179.7377343	-3.0509290	-2.7377370	1.4511620
9	C	1	3	5	1.4111651	108.3618319	0.8395217	-1.0263650	-1.8213200	1.6509040
10	H	9	1	3	1.0812039	125.7195608	176.9936500	-0.3635440	-2.6450320	1.4246990
11	Cr	5	3	1	2.1426299	71.3844638	-64.5821906	-1.8584710	-0.4501550	0.0866030
12	O	11	5	3	2.9817663	95.2370690	-166.5396962	-4.0348290	-1.6578000	-1.5553440
13	O	11	5	3	2.9857190	91.8642297	-86.4853591	-3.3275460	2.0177180	-0.7294480
14	C	12	11	5	1.1519106	1.2825863	-177.8488566	-3.1792610	-1.1899960	-0.9421060
15	C	13	11	5	1.1511076	1.2012657	162.5815379	-2.7443460	1.0710780	-0.4314560
16	S	11	5	3	2.3481744	152.6114565	98.8900385	-0.3413480	-1.2891360	-1.4971810
17	N	16	11	5	1.6894978	59.0786013	-130.4114685	-0.2307490	0.3049530	-0.9485000
18	N	17	16	11	2.3808910	89.7883720	132.9841330	2.1113070	0.0223720	-0.6266870
19	N	16	11	5	1.6991374	112.8837116	-35.3382795	0.9672020	-2.1094590	-0.7887780
20	C	18	17	16	1.3301355	27.2840882	172.8840670	1.0027890	0.7567520	-0.6603680
21	C	19	16	11	1.2958348	112.3763679	-90.0987416	1.9651530	-1.3220750	-0.5371670
22	C	20	18	17	1.4750012	117.3542545	178.6352438	1.1274180	2.1878010	-0.3254130
23	C	22	20	18	1.3995868	121.0753950	161.0582594	0.1407190	3.1063790	-0.7015550
24	C	22	20	18	1.4003589	119.3217713	-18.3652522	2.2583450	2.6334020	0.3698920
25	C	23	22	20	1.3886492	120.0975819	179.8676624	0.2774180	4.4487020	-0.3731820
26	H	23	22	20	1.0834639	119.4733670	-1.7639551	-0.7147830	2.7658480	-1.2725620
27	C	24	22	20	1.3879253	120.0735399	-179.8440381	2.3900760	3.9760420	0.6959310
28	H	24	22	20	1.0840967	118.4873845	0.0874574	3.0164910	1.9081890	0.6429240
29	C	25	23	22	1.3931467	120.0503321	0.1800068	1.3993390	4.8845320	0.3283900
30	H	25	23	22	1.0853984	119.7552104	179.5775347	-0.4878000	5.1574010	-0.6736430
31	H	27	24	22	1.0855136	119.8153538	179.7518228	3.2665570	4.3162170	1.2385190
32	H	29	25	23	1.0859501	119.9328289	179.9160237	1.5049530	5.9349160	0.5830010
33	C	21	19	16	1.5305143	115.4872697	-177.3048888	3.2085400	-1.9996840	0.0436160
34	F	33	21	19	1.3286949	112.3707029	5.9494291	3.0946880	-3.3230970	0.0759580
35	F	33	21	19	1.3334052	110.5321332	127.2655352	4.2892040	-1.6862670	-0.6718590
36	F	33	21	19	1.3425789	109.4848279	-113.9965551	3.4066810	-1.5705490	1.3002390

Table S7. RB3PW91/ 6-31G(2d,p) Geometry and Cartesian Coordinates for **5a⁻**.

Label	Symbol	NA	NB	NC	Bond	Angle	Dihedral	X	Y	Z
1	S							-1.1264900	2.5809630	-0.1422570
2	N	1			1.7373365			-2.2260320	1.2683150	0.1515130
3	N	2	1		2.4273766	87.7447840		-0.4295460	-0.2463380	-0.4572740
4	N	1	2	3	1.7274990	105.5822080	-26.0924793	0.4528890	1.9292840	0.1129470
5	C	2	1	4	1.2925307	111.5698975	-28.5440126	-1.6824020	0.1253500	-0.1106570
6	C	4	1	2	1.3008741	113.8296993	29.6126905	0.5466310	0.6592560	-0.1525990
7	C	5	2	1	1.5255351	114.6525409	-178.2422246	-2.6021660	-1.0761870	0.0832510
8	F	7	5	2	1.3491033	111.7722577	-110.0094380	-2.2343310	-1.8216190	1.1458460
9	F	7	5	2	1.3470508	111.2636505	131.1596511	-2.5687490	-1.8946040	-0.9861520
10	F	7	5	2	1.3398016	113.4818256	10.7251967	-3.8853450	-0.7410350	0.2734960
11	C	6	4	1	1.4955722	115.4247460	174.9272761	1.9236740	0.0834500	-0.0580680
12	C	11	6	4	1.3992451	121.1372091	-4.9488891	3.0329620	0.8983490	0.1935400
13	H	12	11	6	1.0850260	117.8357044	0.5142475	2.8609640	1.9613750	0.3264830
14	C	12	11	6	1.3891529	120.6528392	-179.5717606	4.3087160	0.3540440	0.2705430
15	H	14	12	11	1.0876374	119.7706107	-179.8213677	5.1605040	1.0003810	0.4696930
16	C	14	12	11	1.3952672	120.2787887	0.2759884	4.5009010	-1.0162850	0.0915630
17	H	16	14	12	1.0874208	120.2402343	179.8890939	5.5000480	-1.4414350	0.1501870
18	C	16	14	12	1.3921167	119.4057610	-0.0600858	3.4027260	-1.8329380	-0.1635420
19	H	18	16	14	1.0876416	119.9573805	-179.9728224	3.5421830	-2.9024100	-0.3040610
20	C	18	16	14	1.3919925	120.3187317	-0.1895548	2.1237080	-1.2883580	-0.2355750
21	H	20	18	16	1.0846517	122.2011466	-179.5804562	1.2462660	-1.8969010	-0.4259440

Table S8. UB3PW91/ 6-31G(2d,p) Geometry and Cartesian Coordinates for **5a·**.

Label	Symbol	NA	NB	NC	Bond	Angle	Dihedral	X	Y	Z
1	S							-1.0535600	2.5292750	-0.0034900
2	N	1			1.6518632			-2.1671410	1.3091990	-0.0055020
3	N	2	1		2.4065571	90.9178268		-0.4158670	-0.3414150	-0.0000260
4	N	1	2	3	1.6402043	109.4108754	0.0497653	0.4565180	1.8890200	-0.0006190
5	C	2	1	4	1.3096008	115.7415232	0.0788206	-1.6792900	0.0938600	-0.0028890
6	C	4	1	2	1.3273734	118.5596307	-0.0167961	0.5856610	0.5679440	0.0000470
7	C	5	2	1	1.5316509	115.8093404	179.7499136	-2.7104970	-1.0386370	0.0012690
8	F	7	5	2	1.3274812	111.9578520	1.4196979	-3.9547850	-0.5770770	-0.0289990
9	F	7	5	2	1.3366778	109.8986309	-119.1385338	-2.5630110	-1.7841910	1.1008620
10	F	7	5	2	1.3361273	110.0386418	122.1044461	-2.5267050	-1.8290810	-1.0601710
11	C	6	4	1	1.4753197	116.8110203	179.9094753	1.9608780	0.0337660	0.0005650
12	C	11	6	4	1.4004681	120.4826527	0.3175469	3.0600820	0.9015330	0.0070390
13	H	12	11	6	1.0841421	119.0979626	0.0405235	2.8868970	1.9717400	0.0123380
14	C	12	11	6	1.3870866	120.0956002	-179.9639211	4.3496320	0.3905830	0.0067220
15	H	14	12	11	1.0854630	119.8042359	-179.9855826	5.1981620	1.0674870	0.0119930
16	C	14	12	11	1.3939974	120.0867940	0.0190897	4.5550140	-0.9881830	-0.0004440
17	H	16	14	12	1.0859103	119.9415340	179.9847273	5.5655770	-1.3856290	-0.0009270
18	C	16	14	12	1.3926552	120.0524764	-0.0147362	3.4654890	-1.8555820	-0.0069910
19	H	18	16	14	1.0854344	120.1306903	179.9909934	3.6239440	-2.9293730	-0.0127220
20	C	18	16	14	1.3885174	120.1174819	-0.0060595	2.1723290	-1.3498970	-0.0062730
21	H	20	18	16	1.0836309	121.1501109	179.9990418	1.3125390	-2.0094360	-0.0113170

Table S9. RB3PW91/ 6-31G(2d,p) Geometry and Cartesian Coordinates for **5a**[+].

Label	Symbol	NA	NB	NC	Bond	Angle	Dihedral	X	Y	Z
1	S							-1.0099620	2.4406410	0.0001500
2	N	1			1.5696559			-2.1023820	1.3135040	0.0006320
3	N	2	1		2.3935984	90.7109137		-0.4043910	-0.3735460	-0.0008950
4	N	1	2	3	1.5629118	112.4757821	-0.0095761	0.4429140	1.8645820	-0.0007190
5	C	3	2	1	1.3028206	26.6792560	-179.9632774	-1.6424910	0.0319780	-0.0003430
6	C	3	2	1	1.3611122	94.7958967	0.0308737	0.6323130	0.5084240	-0.0006640
7	C	5	3	2	1.5397113	118.5351046	-179.9676921	-2.7625100	-1.0245580	-0.0000500
8	F	7	5	3	1.3273509	108.3662759	120.4302143	-3.5041300	-0.8475790	1.0864760
9	F	7	5	3	1.3170430	110.7435486	-0.2454908	-2.2566880	-2.2405820	-0.0057050
10	F	7	5	3	1.3272471	108.3968742	-120.9463322	-3.5120410	-0.8407260	-1.0798620
11	C	6	3	2	1.4295391	119.3343073	179.9558768	1.9732660	0.0130180	-0.0004010
12	C	11	6	3	1.4147584	120.2641486	-179.9948764	3.0655650	0.9121420	-0.0000490
13	H	12	11	6	1.0838279	119.8854767	-0.0091232	2.8853020	1.9808740	-0.0001280
14	C	12	11	6	1.3804107	119.6110514	179.9900269	4.3548970	0.4190330	0.0004110
15	H	14	12	11	1.0842557	120.0783962	-179.9991389	5.1976160	1.1012610	0.0006970
16	C	14	12	11	1.3985633	119.8240637	0.0006300	4.5711380	-0.9627120	0.0005120
17	H	16	14	12	1.0857300	119.4957389	-179.9996039	5.5874380	-1.3447380	0.0008810
18	C	16	14	12	1.3989436	120.9902898	0.0010046	3.4976800	-1.8597800	0.0001320
19	H	18	16	14	1.0843056	120.0748249	179.9986239	3.6824260	-2.9282310	0.0001940
20	C	18	16	14	1.3807253	119.8914934	-0.0009598	2.2020760	-1.3824830	-0.0003310
21	H	20	18	16	1.0835436	120.9659959	179.9984559	1.3577520	-2.0615880	-0.0006550

Table S10. RB3PW91/ 6-31G(2d,p) Geometry and Cartesian Coordinates for **6b**-*exo*.

Label	Symbol	NA	NB	NC	Bond	Angle	Dihedral	X	Y	Z
1	Cr							-1.3025560	-1.6505230	0.1278060
2	S	1			2.3020808			-1.7876310	-0.1270450	-1.5284830
3	N	2	1		1.6923465	60.8589895		-0.1807700	-0.3249040	-1.0356480
4	N	3	2	1	2.4042691	89.8305535	-122.6391426	-0.0656500	2.0151740	-0.4959330
5	N	2	1	3	1.6927860	111.9010918	-99.1138601	-2.3547270	1.3362960	-0.8940070
6	F	5	2	1	2.5940092	177.1708414	164.8980078	-3.2028260	3.6326870	-0.0359860
7	F	4	3	2	2.8234898	131.5013050	60.5993470	-1.5324060	3.5875700	1.3339010
8	F	4	3	2	2.7687024	146.8657847	-8.4899241	-1.3068500	4.4869590	-0.6200870
9	O	1	3	2	2.9767080	120.1809871	-51.1913747	-3.7009050	-0.6855470	1.6034530
10	O	1	3	2	2.9822381	89.1374598	-129.9138795	0.0339480	-0.5712040	2.5655450
11	C	1	3	2	2.2643136	87.1813224	113.6658455	-0.2276040	-3.3283940	-0.9475280
12	H	11	1	3	1.0803023	123.2236349	11.1114998	0.6335830	-3.1699580	-1.5802270
13	C	11	1	3	1.4155217	68.8666267	130.9300624	-0.2017340	-3.5216410	0.4545020
14	H	13	11	1	1.0807751	126.0038677	-120.5061919	0.6840110	-3.5976370	1.0691200
15	C	13	11	1	1.4257723	107.8938516	61.1487978	-1.5492860	-3.6369200	0.9057680
16	H	15	13	11	1.0806006	126.1044075	177.5861780	-1.8667410	-3.8271660	1.9210150
17	C	15	13	11	1.4248298	107.6735602	-1.2958001	-2.3995510	-3.4822310	-0.2270430
18	H	17	15	13	1.0808293	126.0943800	178.6221788	-3.4789330	-3.5381220	-0.2253870
19	C	11	1	3	1.4113768	70.7000049	-109.3427796	-1.5738260	-3.2907620	-1.3697300
20	H	19	11	1	1.0815531	125.9803601	120.7026689	-1.9175630	-3.1460820	-2.3849490
21	C	9	1	3	1.1518640	1.3214477	4.1215608	-2.7701480	-1.0348240	1.0216560
22	C	10	1	21	1.1511975	1.7656360	-97.7842717	-0.4739460	-0.9577780	1.6074950
23	C	4	3	2	1.3196984	27.0583366	-173.3412057	0.4658800	0.8171720	-0.6504350
24	C	5	2	1	1.2907874	113.9241352	82.9013458	-1.4187440	2.1392900	-0.5128660
25	C	23	4	3	1.4659375	117.2670504	179.8942837	1.9014410	0.6803010	-0.3869890
26	C	25	23	4	1.3973001	121.4823641	-164.7684687	2.6180040	-0.4408420	-0.8136310
27	H	26	25	23	1.0837636	118.8977502	1.4299569	2.1000540	-1.2124090	-1.3712650
28	C	26	25	23	1.3876430	121.2333387	179.8028464	3.9776910	-0.5632020	-0.5649700
29	H	28	26	25	1.0831741	119.5881845	-179.2387216	4.5094680	-1.4380700	-0.9186440
30	C	28	26	25	1.3992952	119.4491810	0.0840189	4.6446830	0.4535570	0.1273810
31	C	30	28	26	1.4028582	119.7859545	-0.3921489	3.9362060	1.5865180	0.5545470
32	H	31	30	28	1.0845332	118.3839808	-179.9930155	4.4757120	2.3607250	1.0891020
33	C	31	30	28	1.3780355	120.2123709	0.2546590	2.5866500	1.6976030	0.2989290
34	H	33	31	30	1.0838435	120.8993333	179.8291827	2.0278580	2.5667020	0.6262440
35	C	24	5	2	1.5295988	115.6879783	179.0596464	-1.8859080	3.4839720	0.0468310
36	O	30	28	26	1.3476142	124.5616501	179.8637886	5.9586640	0.4401750	0.4262770
37	C	36	30	28	1.4139784	118.2986348	-0.8290678	6.7242200	-0.6816300	0.0328150
38	H	37	36	30	1.0967584	111.4926816	62.0446980	6.7344490	-0.7986760	-1.0576320
39	H	37	36	30	1.0906783	105.9720166	-179.2528830	7.7393730	-0.4897670	0.3824320
40	H	37	36	30	1.0966913	111.4484111	-60.5184797	6.3511120	-1.6037040	0.4946610

Table S11. RB3PW91/ 6-31G(2d,p) Geometry and Cartesian Coordinates for **6b**-*endo*.

Label	Symbol	NA	NB	NC	Bond	Angle	Dihedral	X	Y	Z
1	C							0.9608750	-0.5222360	1.9587580
2	H	1			1.0811851			0.3623850	0.3773410	1.9979000
3	C	1	2		1.4214776	125.7919011		0.4734640	-1.8512960	2.0877100
4	H	3	1	2	1.0805917	125.9749338	-3.4753000	-0.5485330	-2.1354110	2.2938150
5	C	3	1	2	1.4273570	107.7706600	178.8428419	1.5837660	-2.7377250	1.9505200
6	H	5	3	1	1.0808175	126.1517218	177.9287969	1.5531150	-3.8151560	2.0303280
7	C	5	3	1	1.4229838	107.6164426	-1.1680538	2.7408170	-1.9448240	1.7108870
8	H	7	5	3	1.0808567	126.0666332	179.5672002	3.7467870	-2.3137390	1.5688400
9	C	1	3	5	1.4109519	108.3833012	0.8418891	2.3511610	-0.5788720	1.7249150
10	H	9	1	3	1.0812030	125.7894543	176.9141561	2.9959640	0.2686750	1.5381180
11	Cr	5	3	1	2.1421075	71.5113685	-64.5034016	1.3067320	-1.7037340	0.0950580
12	O	11	5	3	2.9819237	94.4422605	-165.2684278	3.0450280	-3.5579680	-1.4644330
13	O	11	5	3	2.9844317	92.7959129	-85.2183085	-0.7353450	-3.6601870	-0.8583810
14	C	12	11	5	1.1521456	1.2659360	-174.3176470	2.3711220	-2.8267760	-0.8824980
15	C	13	11	5	1.1519711	1.1536653	165.8783199	0.0464720	-2.8904480	-0.5072380
16	S	11	5	3	2.3447772	152.4467086	101.8966284	1.8655140	-0.0426740	-1.4627040
17	N	16	11	5	1.6877881	59.3455895	-131.3828204	0.2637920	-0.2654330	-0.9794920
18	N	17	16	11	2.3845424	89.7340357	132.1273476	0.0544300	2.0839140	-0.6290940
19	N	16	11	5	1.6972694	113.0500266	-35.7817344	2.3785290	1.4033450	-0.7370540
20	C	18	17	16	1.3322015	27.3780834	173.1966020	-0.4411300	0.8491820	-0.6970500
21	C	19	16	11	1.2970393	112.4220995	-89.7478525	1.3952270	2.2170950	-0.5063180
22	C	20	18	17	1.4662638	117.3102095	178.9034221	-1.8710740	0.6819570	-0.4191550
23	C	22	20	18	1.3978495	121.5557063	163.6102665	-2.5560880	-0.4806970	-0.7838120
24	C	22	20	18	1.4052722	119.7311070	-15.6340001	-2.5833580	1.7145580	0.2142300
25	C	23	22	20	1.3877367	121.1248311	-179.9458565	-3.9099070	-0.6290490	-0.5173930
26	H	23	22	20	1.0835364	119.3974190	-1.5909047	-2.0265220	-1.2681220	-1.3068540
27	C	24	22	20	1.3787127	120.6608337	-179.9899551	-3.9282950	1.5776440	0.4848730
28	H	24	22	20	1.0841042	118.4384747	-0.1145154	-2.0499690	2.6184100	0.4859460
29	C	25	23	22	1.3992520	119.5543245	0.1521878	-4.6041480	0.4025550	0.1242680
30	H	25	23	22	1.0830435	119.3855188	179.3389543	-4.4150580	-1.5373640	-0.8219740
31	H	27	24	22	1.0846054	121.4076471	179.7081684	-4.4887450	2.3648840	0.9773340
32	C	21	19	16	1.5305015	115.4156724	-176.7089971	1.7902420	3.5763340	0.0758050
33	F	32	21	19	1.3291104	112.3775516	4.7757670	3.1081710	3.7296930	0.1537700
34	F	32	21	19	1.3340854	110.5002507	125.9986993	1.2945330	4.5656300	-0.6694130
35	F	32	21	19	1.3422064	109.6424577	-115.2351933	1.2861590	3.7007820	1.3135170
36	O	29	25	23	1.3477806	124.5735448	-179.9636848	-5.9158190	0.3658280	0.4319740
37	C	36	29	25	1.4144849	118.2491228	0.3863029	-6.6504270	-0.7948450	0.0943990
38	H	37	36	29	1.0966084	111.4693368	-61.7780946	-6.6582460	-0.9639060	-0.9890710
39	H	37	36	29	1.0966157	111.4671876	60.7530500	-6.2511860	-1.6831990	0.5983830
40	H	37	36	29	1.0906781	105.9532693	179.5120339	-7.6700550	-0.6144960	0.4370530

Table S12. RB3PW91/ 6-31G(2d,p) Geometry and Cartesian Coordinates for **5b⁻**.

Label	Symbol	NA	NB	NC	Bond	Angle	Dihedral	X	Y	Z
1	S							-2.3180910	2.4540370	-0.1399440
2	N	1			1.7365698			-3.1483310	0.9577460	0.1558420
3	N	2	1		2.4274476	87.7709696		-1.1011210	-0.1908200	-0.4624050
4	N	1	2	3	1.7284524	105.5904445	-26.1132122	-0.6420780	2.1123410	0.1085960
5	C	2	1	4	1.2927650	111.5845368	-28.5332776	-2.3996170	-0.0621290	-0.1097210
6	C	4	1	2	1.3010446	113.7925163	29.6863552	-0.3114210	0.8831940	-0.1608120
7	C	5	2	1	1.5252716	114.6208057	-178.3504490	-3.0751520	-1.4151820	0.0886560
8	C	6	4	1	1.4927800	115.5015597	174.9282823	1.1467710	0.5759690	-0.0731710
9	C	8	6	4	1.4011492	121.4103284	-4.8582304	2.0907730	1.5802670	0.1787510
10	H	9	8	6	1.0850434	117.9022667	0.4305502	1.7292100	2.5939890	0.3164430
11	C	9	8	6	1.3839735	121.0968193	-179.6719095	3.4418130	1.2892230	0.2520100
12	H	11	9	8	1.0860837	121.4268728	-179.8511814	4.1779090	2.0630420	0.4493540
13	C	11	9	8	1.3988430	120.1127719	0.3316585	3.8879610	-0.0235700	0.0668390
14	C	13	11	9	1.3929620	119.6258556	-0.1140948	2.9648820	-1.0349120	-0.1890040
15	H	14	13	11	1.0846032	121.0608908	-179.9429671	3.2849830	-2.0608220	-0.3353190
16	C	8	6	4	1.3931166	120.4433082	175.7167441	1.6057140	-0.7269570	-0.2535290
17	H	16	8	6	1.0847700	117.2564098	-0.8412622	0.8622230	-1.4938040	-0.4429830
18	C	13	11	9	2.3668456	147.5962980	179.2463497	5.7234190	-1.5141510	-0.0390870
19	H	18	13	11	1.0991510	94.9299684	-124.8069837	5.4743790	-1.8998300	-1.0377680
20	H	18	13	11	1.0991836	95.3021851	126.1014865	5.3298240	-2.2134780	0.7120650
21	H	18	13	11	1.0931085	137.4481086	0.4182631	6.8106720	-1.4610660	0.0606580
22	O	13	11	9	1.3706829	115.7505758	179.8083668	5.2431020	-0.2098970	0.1542850
23	F	7	5	2	1.3471904	111.3303473	131.6678525	-2.8850710	-2.2185730	-0.9759350
24	F	7	5	2	1.3495211	111.7740711	-109.5021948	-2.5752680	-2.0725950	1.1559570
25	F	7	5	2	1.3398779	113.4863963	11.1952717	-4.3990720	-1.3287010	0.2758180

Table S13. UB3PW91/ 6-31G(2d,p) Geometry and Cartesian Coordinates for **5b˙**.

Label	Symbol	NA	NB	NC	Bond	Angle	Dihedral	X	Y	Z
1	S							2.2150400	2.4329630	-0.0125420
2	N	1			1.6509743			3.0950760	1.0361090	-0.0197410
3	N	2	1		2.4068991	90.8814259		1.0787600	-0.2780780	0.0036130
4	N	1	2	3	1.6388990	109.5772717	-0.1842633	0.6158790	2.0744700	-0.0000250
5	C	2	1	4	1.3106552	115.6286221	-0.2763574	2.3975280	-0.0734510	-0.0087670
6	C	4	1	2	1.3306647	118.5335797	0.0681996	0.2513840	0.7947060	0.0039860
7	C	5	2	1	1.5312309	115.7378340	-179.2848438	3.2113800	-1.3704480	0.0018050
8	C	6	4	1	1.4659683	116.9319523	-179.6609295	-1.1874800	0.5141330	0.0074730
9	C	8	6	4	1.4051170	120.9985516	-0.5702048	-2.1282490	1.5577730	0.0185640
10	H	9	8	6	1.0842472	119.0737365	-0.1836151	-1.7771260	2.5835520	0.0276240
11	C	9	8	6	1.3780903	120.6458004	179.8013303	-3.4792210	1.2857310	0.0176650
12	H	11	9	8	1.0845386	121.4316336	179.9966525	-4.2163330	2.0812290	0.0261980
13	C	11	9	8	1.4033453	120.1822312	-0.0603231	-3.9314060	-0.0427000	0.0043290
14	C	13	11	9	1.3987275	119.7589444	0.0986881	-3.0056080	-1.0911420	-0.0059720
15	H	14	13	11	1.0830491	120.9855212	179.9757738	-3.3325600	-2.1236140	-0.0159400
16	C	14	13	11	1.3873739	119.5834495	-0.0456742	-1.6478530	-0.8060050	-0.0038510
17	H	16	14	13	1.0838496	120.2692119	-179.9651989	-0.9207960	-1.6097750	-0.0123240
18	C	13	11	9	2.3714041	147.2741621	-179.5709925	-5.7878580	-1.5180440	-0.0181100
19	H	18	13	11	1.0965976	95.4515423	-125.2593744	-5.4823480	-2.0834430	0.8704360
20	H	18	13	11	1.0965813	95.2152805	124.6440478	-5.4745770	-2.0587630	-0.9192030
21	H	18	13	11	1.0906662	135.9662200	-0.1576849	-6.8733910	-1.4123990	-0.0212800
22	O	13	11	9	1.3473348	115.5834578	-179.8786599	-5.2693010	-0.2018940	0.0020260
23	F	7	5	2	1.3378136	109.8676440	116.1583590	2.9847510	-2.0401610	1.1375290
24	F	7	5	2	1.3362652	110.2342540	-125.1131223	2.8447220	-2.1544450	-1.0162890
25	F	7	5	2	1.3279369	112.0354317	-4.3131653	4.5157710	-1.1409340	-0.0946510

Table S14. RB3PW91/ 6-31G(2d,p) Geometry and Cartesian Coordinates for **5b**[+].

Label	Symbol	NA	NB	NC	Bond	Angle	Dihedral	X	Y	Z
1	S							-2.1390280	2.3621800	0.0049670
2	N	1			1.5684598			-3.0290980	1.0707420	0.0103970
3	N	2	1		2.3976839	90.6094605		-1.0695980	-0.3108310	-0.0120450
4	N	1	2	3	1.5600013	112.9143243	-0.1368411	-0.6112730	2.0468700	-0.0072070
5	C	3	2	1	1.2965575	26.6436617	-179.5950811	-2.3517430	-0.1182490	-0.0032360
6	C	3	2	1	1.3705546	94.7628936	0.3783145	-0.1895300	0.7398310	-0.0089570
7	C	5	3	2	1.5371682	118.5259961	-179.6674534	-3.2782900	-1.3447840	-0.0003100
8	C	6	3	2	1.4142148	119.4910958	179.4769095	1.2011850	0.4830930	-0.0079430
9	C	8	6	3	1.4230172	121.0428536	-179.9776151	2.1441460	1.5488270	-0.0042790
10	H	9	8	6	1.0839038	119.6236755	-0.1424879	1.7935200	2.5744530	-0.0045710
11	C	9	8	6	1.3653333	120.3386780	179.8424931	3.4836370	1.2844760	-0.0001040
12	H	11	9	8	1.0838892	121.7741281	-179.9868314	4.2219840	2.0779810	0.0029530
13	C	11	9	8	1.4173163	120.1221178	-0.0066106	3.9440920	-0.0559590	0.0007490
14	C	13	11	9	1.4144511	120.1793082	0.0551633	3.0187040	-1.1256820	-0.0038960
15	H	14	13	11	1.0824715	120.6721766	179.9503479	3.3615590	-2.1524220	-0.0040900
16	C	14	13	11	1.3718637	119.4630249	-0.0462204	1.6739100	-0.8545360	-0.0082610
17	H	16	14	13	1.0838729	120.1570717	179.9936879	0.9549220	-1.6655990	-0.0119470
18	C	13	11	9	2.3856822	146.4862723	-179.8960791	5.8360520	-1.5091990	0.0085320
19	H	18	13	11	1.0935038	95.5507878	-124.2822556	5.5509300	-2.0588630	-0.8927590
20	H	18	13	11	1.0935041	95.5011093	124.2214172	5.5418720	-2.0594700	0.9065360
21	H	18	13	11	1.0885445	133.6293946	-0.0005819	6.9116450	-1.3418700	0.0139970
22	O	13	11	9	1.3151155	115.2782348	-179.9426564	5.2512040	-0.2007300	0.0060660
23	F	7	5	3	1.3279968	108.7734276	-123.3955804	-4.0949100	-1.2660100	-1.0445810
24	F	7	5	3	1.3188618	110.9164993	-2.5921835	-2.5804970	-2.4621490	-0.0633730
25	F	7	5	3	1.3290227	108.4586935	117.9557330	-3.9962390	-1.3271320	1.1179650